THE IMPACT OF WIND GENERATION, DEFERRABLE DEMAND, AND UTILITY-SCALE STORAGE ON SYSTEM COSTS AND CUSTOMERS' PAYMENTS FOR ELECTRICITY

A Dissertation

Presented to the Faculty of the Graduate School

of Cornell University

in Partial Fulfillment of the Requirements for the Degree of

Doctor of Philosophy

by

Wooyoung Jeon

August 2014

THE IMPACT OF WIND GENERATION, DEFERRABLE DEMAND, AND UTILITY-SCALE STORAGE ON SYSTEM COSTS AND CUSTOMERS' PAYMENTS FOR ELECTRICITY

Wooyoung Jeon, Ph.D.

Cornell University 2014

The recent rapid increase in the penetration of renewable sources of generation in electricity markets has introduced a new challenge for system operators due to the inherent variability of these sources. An effective solution to this challenge is to use storage capacity to offset the variabilty. An additional advantage of storage is that it can also shift load from peak to off-peak periods and lower system costs. Since electric batteries are relatively expensive, a promising form of storage is to use deferrable demand devices to decouple the purchase of electricity from the delivery of an energy service, such as thermal storage for space conditioning and hot water. The smart-charging of electric vehicles represents another type of deferrable demand. Two additional advantages of deferrable demand are that it is relatively inexpensive and the potential amount of capacity is enormous.

The objective of this dissertation is to evaluate how high penetrations of wind generation affect the costs of operating an electricity grid and to determine the economic value of different types of storage from the perspective of a system operator and of individual customers. The empirical analysis is based on a stochastic form of multi-period Security-Constrained Optimal Power Flow (SCOPF) using a reduction of the network in New York State and New England. In this model, the potential wind generation and electric load are both

stochastic inputs, and the optimal dispatch of conventional generating units for both energy and reserves over 24 hours is determined endogenously to meet load and maintain system reliability. The results for a hot summer day show that adding wind capacity displaces fossil fuels and increases ramping requirements, but the net effect is lower operating costs. Energy storage reduces operating costs further by 1) buying more energy when electricity prices are low by shifting demand from peak to off-peak hours, 2) providing ancillary services such as ramping services to mitigate the variability of wind generation, and 3) lowering the amount of conventional generating capacity needed to maintain system adequacy at the system peak. This is true for both utility-scale storage and deferrable demand. Although utility-scale storage reduces the operating costs more than the same capacity of deferrable demand, the capital costs of storage are higher and the total of all costs are lower for deferrable demand.

Customers with thermal storage for space and/or water heating get most of their savings from lower demand payments (i.e. reducing their demand at the system peak), and for customers with electric vehicles, the main savings are from buying less gasoline. However, encouraging customers to adopt deferrable demand devices will require charging them an efficient rate structure that reflects the true cost of supplying electricity. Comparing the bills paid by customers with different types of deferrable demand shows that an efficient rate structure provides positive economic incentives for investing in deferrable demand but a flat rate structure for energy only provides perverse incentives.

BIOGRAPHICAL SKETCH

Wooyoung Jeon was born in Busan, South Korea on November 11, 1981. He received a Bachelor in Science with a concentration in Industrial Engineering from Korea Advanced Institute of Science and Technology (KAIST) in 2007. During the time of undergraduate study, he served a military service in 25th Transportation Battalion in Daegu, South Korea and retired as a sergeant in 2005. After finishing his undergraduate study, he worked at ABN AMRO Securities in the Equity Research Team in Seoul, South Korea. He earned a Master of Engineering with a concentration in Financial Engineering from Cornell University in 2009, and then he started the Ph.D program in the Field of Economics at Cornell University. His doctoral research focuses on the Electricity Market and Smart Grid Environment, especially the Integration of renewable energy sources into electricity markets and the evaluation of the true value of various energy storages. He is expecting to finish his Ph.D studies in 2014.

I would like to dedicate this doctoral dissertation to my family. Without the continued support and sacrifice of my parents, Hookeun Jeon and Soonsik Noh, there is no doubt in my mind that I could not complete this program. I would also like to thank my wife, Jung Youn Mo, who has stayed next to me all the time and encouraged me to finish this program.

ACKNOWLEDGEMENTS

Foremost, I would like to express my sincere gratitude to my committee chair, Prof. Tim Mount, who has been a great adviser and respected mentor during my doctoral study. He inspired me to practice the passion and attitude of a true scholar. Besides my advisor, I would also like to show my gratitude to the rest of the committee members, Prof. Max Zhang and Prof. Shanjun Li, for making time to meet with me and sharing thoughtful advice and many insightful comments.

I would also like to thank the members of E3RG including Robert Thomas, Richard Schuler, Lang Tong, Ray Zimmerman, Carlos Murillo-Sanchez, Lindsay Anderson and Eilyan Bitar. From these renowned scholars, I could learn invaluable knowledge and insights about the electricity markets of the past, present and future.

I thank my colleagues and friends, Alberto Lamadrid, Hao Lu, Daniel Munoz, Surin Maneevitjit, Keenan Valentine, John Taber, Santiago Palacio, Monica Nguyen and Jung Youn Mo who shared all the discussions, help and encouragement together during this program.

TABLE OF CONTENTS

LIST OF TABLES

LIST OF FIGURES

CHAPTER 1

THE IMPACT OF DEFERRABLE DEMAND ON SYSTEM COSTS AND CUSTOMERS' PAYMENTS IN THE SMART GRID ENVIRONMENT

1.1 Introduction

With higher penetrations of variable generation from renewable sources, the need to install effective forms of storage capacity on the electric delivery system is critical. However, installing dedicated storage capacity that is designed only to mitigate the variability of generation from a wind farm, for example, is likely to be prohibitively expensive (Tuohy and O'Malley (2011)). A number of studies, including the works of Short and Denholm (2006), Goransson et al. (2010), Wang et al. (2011), Hodge et al. (2010), and Valentine et al. (2011) have shown how the discharging and charging of electric vehicles can be used to smooth daily load cycles as well as provide regulation to support the reliability of supply. If owners of electric vehicles are compensated correctly for providing these services, the overall cost of operating the vehicles is reduced. Since the primary purpose of the batteries in electric vehicles is to provide a means of transportation, the substantial capital cost of a battery is shared between transportation and supporting the grid. This provides a relatively inexpensive form of storage capacity for the grid. (Sioshansi and Denholm (2010)) In spite of this potential, earlier research has shown that the total system effects of high penetrations of electric vehicles are still relatively modest. For example, the reduction of peak system load due to Vehicle-To-Grid(V2G) capabilities is very limited because much of the electric energy stored in the batteries is used for transportation.

The objective of this chapter is to extend the concept of deferrable loads to

include thermal storage, and in particular, the use of ice batteries to replace standard forms of air-conditioning. There has been many papers studied thermal storage. A number of studies including Khudhair and Farid (2004) and Sharma et al. (2009) has analyzed the benefit of thermal storage on heating purpose in the building level, and Hasnain (1998) studied technical characteristics of ice thermal storage with simple examples of optimum operational strategies, and Lee et al. (2009) and Chen et al. (2005a) presented algorithms for optimal operating strategies of Ice storage air conditioning system, but these studies only demonstrated optimum strategies of controlling thermal storage for mostly micro-scale level, and they are not analyzing how the aggregated thermal storage would provide many services and benefit to the whole power system level. Therefore, it is new approach for thermal storage to be seriously considered as a form of deferrable demand in the power system with high penetration of renewable generation to provide regulation services and reduce peak capacity needed for system adequacy.

The information that U.S. Energy Information Administration reported shows that the energy usage for cooling accounts for approximately 30% of energy consumptions in the summer season (EIA (2001)). The econometric analysis of the hourly demand for electricity shows that roughly 38% of the total daily demand for electric energy and 36% of the peak demand for a hot summer day in New York City are temperature sensitive. The potential benefit of this type of storage is that a substantial amount of the peak system load on hot summer afternoons can be moved to off-peak periods at night. Instead of using air-conditioners when space cooling is needed, ice can be made when it is convenient for the electric delivery system. Similar arguments can be made for space heating using oil, for example, to store heat. In this way, thermal storage

can be used to mitigate variable generation, reduce the total amount of generating capacity needed to maintain System Adequacy, and as a result, lower the total operating and capital cost of generating electricity.

This chapter presents an empirical analysis using data for a hot day in New York City to determine the effects of the deferrable demand associated with electric vehicles and thermal storage on total system costs. The results show how a System Operator can optimize the charging of batteries in electric vehicles and the use of thermal storage to make ice. In other words, the daily patterns of conventional (non-controllable) demand and wind generation are taken as exogenous inputs, together with a specified daily pattern of demand for cooling services and a minimum level of electric energy needed for commuting in electric vehicles.

The results show how customers can reduce total system costs by 1) shifting load from expensive peak periods to less expensive off-peak periods, 2) reducing the amount of installed conventional generating capacity needed to maintain System Adequacy, and 3) providing ramping services to mitigate the inherent variability of generation from renewable sources. It is, however, essential to develop a regulatory environment in which all participants in the different markets for electricity and ancillary services, including customers, pay for the services they use and are compensated for the services they provide. This will establish the economic incentives needed to develop a smart grid that customers can afford. The basic argument is that the savings in the total costs of the conventional generation and transmission system will lower customers' bills and help to cover the cost of the investments needed to make the grid smarter.

1.2 Model Specification

1.2.1 The Model of System Costs and Demand

This study is based on an optimization model that assumes the system operator controls all storage to minimize the total system cost of energy and ramping in the electricity market. Some of the generated electricity comes from an exogenous and variable source of wind generation at no cost and the rest comes from a linear supply function representing conventional generating units. Once decisions are made by the system operator, customers pay for both energy and ramping using the optimum marginal prices determined by the system operator. The model was tested in the electricity market for New York City for a hot summer day in 2007.

This study also takes an idea that electricity demand can be divided as Temperature-Sensitive Demand (TSD) and Non-Temperature-Sensitive Demand (N-TSD) presented in Mo (2012). Electricity Demand basically consists of the part that is not affected by temperature such as dish-washing, lighting and other home appliances, and the part that is affected by temperature, and the space cooling mostly by air conditioning during summer season is the dominant element of TSD. The advantage of estimating TSD and N-TSD is that by knowing TSD, we can measure the potential amount of electricity demand that can be shifted from peak hour to off-peak hours by reducing or replacing the use of air conditioning during the summer season. Peak electricity demand on hot summer day usually is the highest electricity demand throughout the whole year and the generating capacity is required to meet this peak demand to maintain system reliability, so reducing summer peak demand enables power

system to save a considerable amount of money by reducing generating capacity required to maintain it. Figure 1.1 shows the daily profile of TSD and N-TSD from the electricity demand of New York City on a hot summer day. TSD is approximately 30% of the total demand at a peak hour.

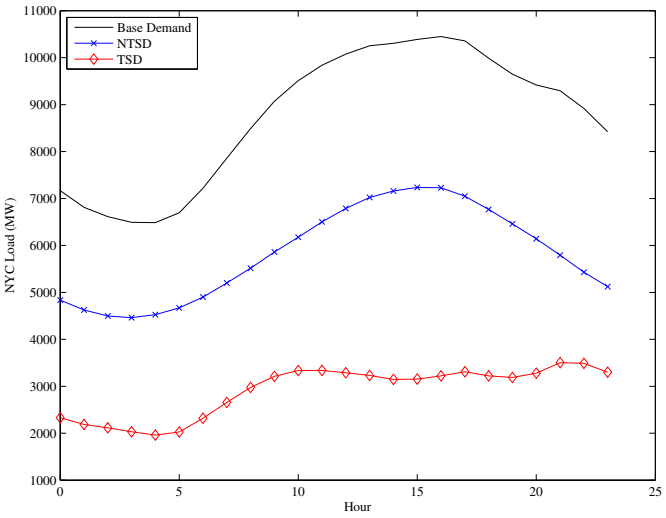

Figure 1.1: Daily profile of Temperature-Sensitive Demand (TSD) and Non Temperature-Sensitive Demand (N-TSD) from Base Demand, Source: Mo (2012)

Given the optimum prices of energy and ramping, I tested the individual payments for four different types of customers, 1) customers with no storage, 2) customers with PHEV, 3) customers with thermal storage, and 4) customers with both types of storage. In computing these payments, not only were traditional energy payment types considered but also ramping payments and capacity payments. The latter payment corresponds to a demand charge that measures the real system cost of ensuring that there is enough generating capacity to maintain reliability. It is possible that ramping payments are negative when customers provide ramping services to mitigate the variability of wind generation. All customers are assumed to have an identical daily pattern of demand for

non-transportation electric energy services. For customers with thermal storage, their demand is divided between air conditioning services and other services.

In addition to these market data, wind capacity and two types of storage, PHEV and thermal storage, were integrated into the system. The type of PHEV was specified using the characteristics of a GM Volt electric car to determine the battery size and performance. The type of thermal storage was specified as an ice battery, which basically makes ice when electricity prices are low and uses the stored ice for cooling to replace a traditional air-conditioner when prices are high. The electricity demand data came from the New York Independent System Operator (NYISO). Wind generation was based on data provided by the National Renewable Energy Laboratory (NREL) to represent the available generation in each hour for 2GW of wind capacity. Based on this assumption, wind generation accounted for 12% of the total daily demand.

Table 1.1: Specification of thermal storage and PHEV

	THERMAL	PHEV
Capacity (GWh)	5	5
Individual storage size (kWh)	20	10
# of Customer with Storage	250,000	500,000
Penetration Rate	6.2%	44.2%
Charging Efficiency	90%	90%
Discharging Efficiency	90%	90%
Charging Speed (kWh/hr)	2 (10%)	3.31 (33%)
Discharging Speed (kWh/hr)	5 (25%)	3.31 (33%)

Table 1.1 summarizes the specification of thermal storage and PHEV. A total

of 10 GWh of customer storage is assumed to be installed with 5 GWh coming from PHEVs and 5 GWh coming from thermal storage. The individual storage size of PHEV is 10 kWh , which is approximately the usable size of the battery in a GM Volt (65% of 16 kWh). Therefore, 5 GWh of PHEV storage corresponds to 500,000 people owning a PHEV. This is 44.2% of the number of commuters representing a very high penetration rate in New York City, (1,130,002 commuters in 2006 according to the New York City Department of City Planning, (2008)). The battery type used in a GM Volt is a lithium-ion battery with a charging and discharging efficiency of 90%. For charging technology, two types of charging levels are considered using current technology. Level 1 chargers deliver up to 1.44 kW and level 2 chargers deliver up to 7.68 kW(The Massachusetts Division of Energy Resources (2000)). It is assumed that 70% of level 1 chargers and 30% of level 2 chargers are available in NYC, which implies an average of 3.31 kW. The specified average driving distances for "rural," "suburban," and "center city" are 36.9 miles, 28.8 miles, and 27.2 miles, respectively (U.S. Department of Energy, Transportation Energy Data Book 29th Edition). Their analysis specifies 27.2 miles as the average driving distance for commuters in New York City. In the current study, the driving patterns of commuters are assumed to be distributed equally from 7am to 9am , and from 4pm to 6pm. At the other times, PHEVs are connected to the grid. PHEVs increase electricity demand due to the energy used for driving, but if they have smart chargers and Vehicle-To-Grid (V2G) capabilities, PHEVs can help to mitigate wind variability and reduce the peak system load. They also reduce gasoline purchases.

Thermal storage of 5 GWh corresponds to only 6.2% of the total TSD estimated by the econometric model described previously. This means that there is considerably more room for thermal storage to expand than there is for PHEVs.

Thermal storage disconnects the timing of the purchase of electricity from the delivery of cooling services. The cooling demand is assumed to be 6.2% of the TSD each hour, and the 2 kWh charging speed is based on the technical capability of a ThermalCUBE ice-battery (www.thermalcube.com). The discharging rate of 5 kWh corresponds to an average household with 1000 ft^2 of residential space. The recommended alternative is to use an 18000 BTU air-conditioner which has an hourly energy consumption level of approximately 5 kWh.

1.2.2 The System Operator's Minimization Problem

The optimization problem is formulated as minimizing the sum of the energy cost and reserve cost for a 24-hour period. Given the deterministic daily profiles of demand and wind generation, the total system cost is determined by the hourly levels of charging or discharging of PHEV (Ph_t) and thermal storage (Th_t) which are controlled by the system operator. In the objective function (1.1), the system operator controls three variables, Ph_t, Th_t^+, and Th_t^-. Charging (making ice) and discharging (melting ice) for thermal storage are separated because the specification of thermal storage from ThermalCUBE can purchase electricity for air conditioning and use a fan to melt ice for cooling at the same time, unlike a PHEV. Hence, the hourly demand for cooling services can be met by a combination of purchasing electricity and melting ice.

The specific form of the optimization model used by the system operator can be found in (1.1) - (1.15), and the definitions of all variables used in the model are described in Table 1.2.

$$\underset{Ph,Th^+,Th^-}{Min} \sum_{t=1}^{24} EnergyCost(CG_t) + ReserveCost(CG_t, |\Delta CG_t|) - P_{FEIS} \cdot FEIS \tag{1.1}$$

subject to:

$$HCL_t^{Th^+} \leq Th_t^+ \leq HCU_t^{Th^+}, \forall t = 1, ..., 24 \tag{1.2}$$

$$HCL_t^{Th^-} \leq Th_t^- \leq HCU_t^{Th^-}, \forall t = 1, ..., 24 \tag{1.3}$$

$$HCL_t^{Ph} \leq Ph_t \leq HCU_t^{Ph}, \forall t = 1, ..., 24 \tag{1.4}$$

$$SCL_t^{Th} \leq Th_{initial} + \sum_{t=1}^{T'} Th_t^+ - \sum_{t=1}^{T'} Th_t^- \leq SCU_t^{Th}, \forall T' = 1, ..., 24 \tag{1.5}$$

$$SCL_t^{Ph} \leq Ph_{initial} + \sum_{t=1}^{T'} Ph_t \leq SCU_t^{Ph}, \forall T' = 1, ..., 24 \tag{1.6}$$

$$\sum_{t=1}^{T'} Th_t^- \leq Th_{initial} + \sum_{t=1}^{T'} Th_t^+, \forall T' = 1, ..., 24 \tag{1.7}$$

$$L_t = L_t^{NC} + L_t^C \tag{1.8}$$

$$L_t^C = C_{Th}^- \cdot Th_t^- + AC_t \tag{1.9}$$

$$C_{Th}^- \cdot Th_t^- \leq L_t^C, \forall t = 1, ..., 24 \tag{1.10}$$

$$\begin{aligned} CG_t &= L_t - W_t + C_{Th}^+ \cdot Th_t^+ - C_{Th}^- \cdot Th_t^- + H_{vac} \cdot C_{Th}^- \cdot Th_t^- + DP \cdot C_{Ph} \cdot Ph_t \\ &= L_t^{NC} + L_t^C - C_{Th}^- \cdot Th_t^- - W_t + C_{Th}^+ \cdot Th_t^+ + H_{vac} \cdot C_{Th}^- \cdot Th_t^- + DP \cdot C_{Ph} \cdot Ph_t \\ &= L_t^{NC} + AC_t - W_t + C_{Th}^+ \cdot Th_t^+ + H_{vac} \cdot C_{Th}^- \cdot Th_t^- + DP \cdot C_{Ph} \cdot Ph_t \end{aligned} \tag{1.11}$$

$$\begin{aligned} EnergyCost &= EP_t \cdot CG_t^{[1]} + RampWearCost(|\Delta CG_t|^2)^{[2]} \\ &= EP_t \cdot CG_t^{[1]} + [\delta \cdot |\Delta CG_t|^2]^{[2]} \end{aligned} \tag{1.12}$$

$$\begin{aligned} ReserveCost &= RampResCost(|\Delta CG_t|)^{[1]} + OpResCost(CG_t)^{[2]} \\ &= [\gamma \cdot |\Delta CG_t|]^{[1]} + [\eta \cdot (\alpha \cdot CG_t)]^{[2]} \end{aligned} \tag{1.13}$$

$$EP_t = \beta_0 + \beta_1 \cdot CG_t \tag{1.14}$$

$$\begin{aligned} FEIS &= Storage\_Level\_at\_Final\_State - Storage\_Level\_at\_Initial\_State \\ &= \sum_{t=1}^{T'} C_{Th}^+ Th_t^+ - \sum_{t=1}^{T'} C_{Th}^- Th_t^- + \sum_{t=1}^{T'} C_{Ph} Ph_t, T' = 24 \end{aligned} \tag{1.15}$$

The objective function (1.1) consists of an energy cost part, a reserve cost part and a part that deals with additional energy for storage. The energy cost

Table 1.2: Definition of Variables

CG_t	Conventional Generation at time t, a function of control variables(Th^+, Th^-, Ph)
$EnergyCost$	Energy cost and Ramp Wear Cost
$ReserveCost$	Ramp Reserve Cost and Operating Reserve Cost
L_t	Base system electricity demand at time t
W_t	Wind generation at time t
Th_t^+	Electricity demand purchased by Thermal storage at time t
Th_t^-	Electricity demand supplied by Thermal storage at time t
$Th_{initial}$	Initial state of Thermal storage
Ph_t	Electricity demand purchased or supplied by PHEV at time t
$Ph_{initial}$	Initial state of PHEV
C_{Th}	Efficiency of Thermal storage
C_{Ph}	Efficiency of PHEV
L_t^{NC}	Electricity demand by non-cooling services at time t, determined by N-TSD
L_t^C	Electricity demand by cooling services at time t, determined by TSD
AC_t	Electricity demand met by air conditioning at time t
$HCL_t^{(\cdot)}$	Hourly power rate lower bound of storage at time t
$HCU_t^{(\cdot)}$	Hourly power rate upper bound of storage at time t
$SCL_t^{(\cdot)}$	Energy capacity lower bound of storage at time t
$SCU_t^{(\cdot)}$	Energy capacity upper bound of storage at time t
EP_t	Energy price at time t
DP	Driving profiles of PHEV owners
$FEIS$	Final Energy in Storage, Storage level at final state - Storage level at initial state
P_{FEIS}	Opportunity cost of FEIS
H_{VAC}	% of energy used for HVAC system when using thermal storage
β	Coefficients estimated from market data
γ, δ, η	Coefficients for ramp reserve cost, ramp wear cost and operating reserve cost
α	Proportion of CG_t required for operating reserve

is a function of conventional generation (CG_t) times the energy price (EP_t) and of ($|\Delta CG_t|^2$) to represent the wear-and-tear cost of providing ramping services.[1]

[1]This is similar to reducing the miles/gallon and the useful engine life for an automobile

Ramp wear-and-tear cost is the cost of the physical stress on generators caused by dispatch changes between consecutive hours. This cost is shown to follow a piecewise linear function in Troy (2011) but for simplicity, I assume this cost has a quadratic form ([2] in (1.12)). The energy price in (1.14) is determined by fitting an AR(2) time-series model of price regressed on load that gave the best fit and satisfied the white noise test. The reserve cost in (1.13) consists of two components, a ramp reserve cost and an operating reserve cost. The ramp reserve cost is the cost of purchasing capacity in advance to make sure that the system can meet the changes of conventional generation between consecutive hours caused by wind variability and the hourly demand profile.[2] The cost function is the ramp reserve offer (γ) times the absolute change of conventional generation between two consecutive hours ([1] in (1.13)). Operating reserve cost is the cost of committing capacity to cover any contingency situation within each hour. The cost function is the operating reserve offer (η) times the operating reserve quantity determined by a ratio parameter (α) ([2] in (1.13)). This reserve cost structure is introduced and tested in Lamadrid et al. (2013). Energy cost and reserve cost are functions of (CG_t), and (CG_t) is defined in (1.11) and determined by the charging and discharging levels of all control variables (Th_t^+, Th_t^-, and Ph_t).

Constraints (1.2), (1.3) and (1.4) define the hourly charging limits which are determined by the charging and discharging speeds specified in Table 1.1. Con-

---

when it accelerates.

[2]In this model, the hourly pattern of wind generation is deterministic, and the ramping reserve capacity purchased in advance is the same as the ramping delivered. However, in a model that treats wind generation as a stochastic input, the reserve capacity purchased would be the maximum ramping that may be needed, and the expected ramping delivered would be less than the reserve capacity.

straints (1.5) and (1.6) define the limits of the storage capacity of thermal storage and PHEV that must be met each hour. Constraint (1.7) implies that the cooling energy discharged at t+1 is limited to the stored energy level at t. Constraint (1.8) specifies that the regular load is divided into L_t^{NC} and L_t^C which indicates Load Not-for-Cooling and Load for Cooling, respectively. As noted previously, L_t^C is proportional to TSD each hour. In constraint (1.9), L_t^C is the cooling demand that can be met by traditional air conditioning (AC_t) and thermal storage (Th_t^-). Constraint (1.10) specifies that cooling by thermal storage cannot exceed the specified cooling demand. In constraint (1.11), CG_t measures the Conventional Generation, which is basically the amount of conventional generating capacity needed to meet the system load when wind generation and the two types of storage are accounted for in the market. Two important assumptions are imposed in CG_t. The first one is that cooling by thermal storage requires additional energy consumption compared to standard HVAC systems that is proportional to 10% of the cooling load supplied by thermal storage. The second one is that when L_t^{NC} is given, the amount of CG_t increases to cover any cooling load supplied by traditional air conditioning. Finally, $FEIS$ in equation (1.1) measures the final additional energy in storage, which is computed as the storage level at the final state minus the storage level at the initial state, and the appropriate value (P_{FEIS}) is assigned to this as the opportunity cost of having additional energy in storage in the terminal state. The value for $FEIS$ is set to the average of the four highest electricity prices.

This study tested two sets of reserve cost parameters for a low ramping cost case and a high ramping cost case, shown in Table 1.3. Parameters for the low ramping cost case are taken from Lamadrid et al. (2013). The ramp wear-and-tear coefficient determined in Lamadrid et al. (2013) is intended to illustrate how

Table 1.3: Cost setup for two ramp cases

	low ramping cost case	high ramping cost case
ramp reserve offer, γ ($/\Delta MW$)	10	10
ramp wear coefficient, δ	0.0028	0.2
operating reserve offer, η ($/MW$)	5	5
% of operating reserve quantity, α	10%	10%

this cost affects system operations rather than to provide an accurate estimate of the cost. The ramp wear-and-tear coefficient in the high ramp case is based on the amount of the system cost reduction demonstrated in Troy (2011) when ramping cost is implemented in the optimization. According to this chapter, the optimum system cost is approximately 14% lower than the system cost when ramping costs are ignored in the optimization.The ramp wear-and-tear coefficient for the high ramp case is determined at the level that shows a similar cost reduction. In the results section, the system level results for both the low and high ramping cost cases are presented to demonstrate the impact of ramp costs on the system cost and pattern of conventional dispatch.

1.3 Results

1.3.1 Total System Cost

Figure 1.2 illustrates the hourly values of the load supplied by conventional generating units for the Base Load (L_t), Net Load ($L_t - W_t$) with wind generation added and the Optimum Load ($L_t - W_t + DeferrableDemand_t$) with PHEV and

thermal storage controlled by the system operator for the two different ramping cost cases. The typical characteristics of wind generation provide more energy in the early morning and less energy during the daytime when energy demand is at its peak. Consequently, the difference between the peak load and the minimum load is even larger for Net Load than it is for the Base Load. This provides a greater incentive for storage to take advantage of the energy cost savings by shifting load from the expensive peak hours to off-peak hours.[3] As a result, the daily profile of the Optimum Load is much flatter in both ramping cost cases. However, there are significant differences in the smoothness of the Optimum Load profiles in the two cases. In the low ramping cost case, the Optimum Load puts more weight on shifting peak load to off-peak hours to maximize the price arbitrage and less weight on smoothing the load profile. In contrast, with the high ramping cost, the Optimum Load puts less weight on benefitting from price arbitrage and more on smoothing the profile to reduce ramping costs.

The Optimum Load profiles allow PHEVs to store energy during off-peak hours and to discharge it during peak hours to benefit from price arbitrage. However, the amount of energy sold back to the grid from 10am to 8pm is not as great as the energy purchased at night because a significant amount of the stored energy is used for commuting. In a similar way, there are efficiency losses for both PHEVs and thermal storage.

[3]It should be noted that even though the addition of deferrable demand increases the total daily amount of energy supplied to customers, the optimum levels of conventional generation fall well within the range of generation with no deferrable demand (i.e. Net Load). Consequently, the existing generating units can meet the optimum load, and in fact, the lower peak for the optimum load implies that less installed capacity is actually needed to maintain system adequacy.

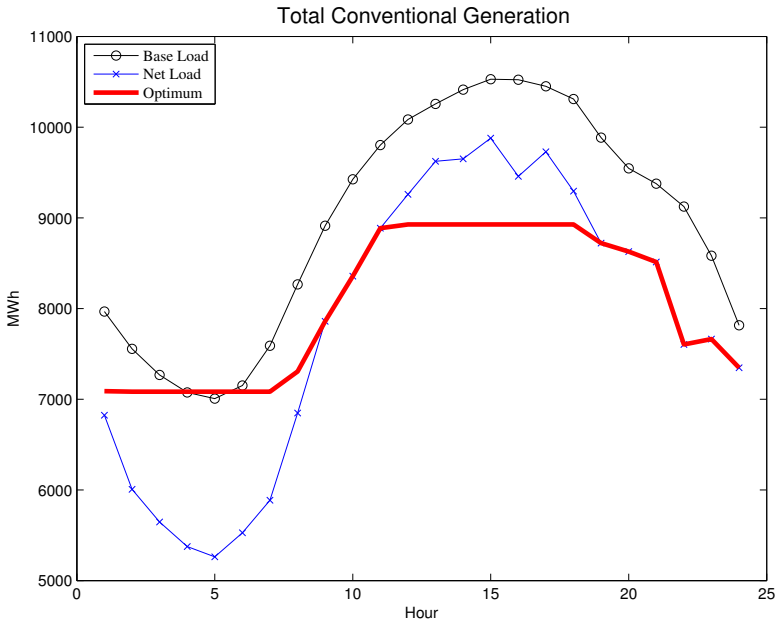

(a) low ramping cost case

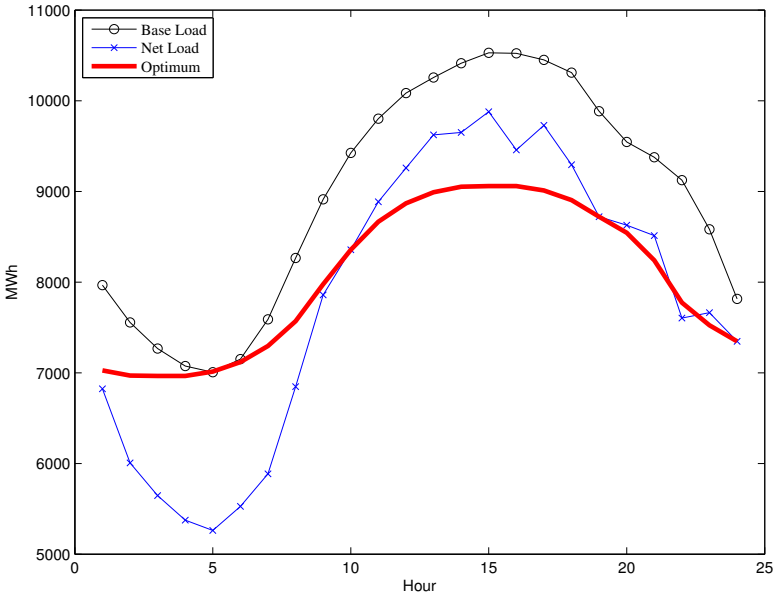

(b) high ramping cost case

Figure 1.2: Optimum load after running optimization with thermal storage and PHEV with two different coefficients of ramp wear cost

Table 1.4: System Costs per day, low ramping cost case

	Base Load	Net Load	Optimum Load
Energy Cost ($1000)*	10,355	6,613	6,789
Reserve Cost($1000)	188	203	137
Total Operating Cost($1000)	10,543	6,816	6,927
Max System Load(MW)	10,529	9,879	8,927
Capacity Cost($1000)**	20,383	19,125	17,282
TOTAL SYSTEM COST($1000)	30,927	25,941	24,209
Total Saving in Gasoline($1000)***	0	0	2,720
TOTAL COST TO CUSTOMERS($1000)	30,927	25,941	21,489
% Cost Reduction from Base Load	-	19.2%	30.5%
% Cost Reduction from Net Load	-	-	17.2%

* Energy Cost includes FEIS, Valued at $120/MWh (Average Peak Price).
** Annual Capital Cost for a Peaker $88k/MW/year allocated to 100 peak hours with 2 peak hours for this day.
***Each vehicle drives 27.2 Miles at 20 Miles/Gal at $4/Gal.

Table 1.4 and Table 1.5 summarize the total system costs for the two different ramping cost cases for the three different load cases, Base Load, Net Load with wind generation added, and Optimum Load with thermal storage and PHEVs. In both tables, the energy costs for Net Load and Optimum Load are roughly two-thirds of the levels for Base Load. This reduction reflects the displacement of fossil fuels by wind generation. The higher energy cost for the Optimum Load compared to the Net Load reflects the increase of demand by PHEVs. However, the effect of this increased demand on the energy cost is small because flattening the daily load profile more reduces the energy price difference between the peak and off-peak hours. Extrapolating this result to a very high penetration of PHEVs and thermal storage, the energy cost reduction of storage is eliminated if the daily load profile is completely flat.

Table 1.5: System Costs per day, high ramping cost case

	Base Load	Net Load	Optimum Load
Energy Cost ($1000)*	10,355	6,613	6,804
Reserve Cost($1000)	826	1,308	349
Total Operating Cost($1000)	11,181	7,920	7,153
Max System Load(MW)	10,529	9,879	9,059
Capacity Cost($1000)**	20,383	19,125	17,539
TOTAL SYSTEM COST($1000)	31,564	27,045	24,692
Total Saving in Gasoline($1000)***	0	0	2,720
TOTAL COST TO CUSTOMERS($1000)	31,564	27,045	21,972
% Cost Reduction from Base Load	-	16.7%	30.4%
% Cost Reduction from Net Load	-	-	18.8%

* Energy Cost includes FEIS, Valued at $120/MWh (Average Peak Price).
** Annual Capital Cost for a Peaker $88k/MW/year allocated to 100 peak hours with 2 peak hours for this day.
***Each vehicle drives 27.2 Miles at 20 Miles/Gal at $4/Gal.

In contrast to the energy costs, the costs of reserves with Net Load increase from the Base Load due to the variability of wind generation. The reserve costs for Optimum Load are lower than the levels for Net load in both the low and high ramping cost cases, but in terms of magnitude, the reduction in the high ramping cost case is much larger and these costs are an important consideration for the system operator. It is clear in the high ramping cost case that the storage can mitigate the ramping for both load-following and the variability of wind generation.

The Optimum Load also has the lowest capacity cost because 10% less conventional generating capacity is needed to meet the peak load. By reducing the peak system load, the amount of installed conventional generating capacity needed to maintain system adequacy is also reduced and the corresponding

capital cost of this capacity is saved. The cost of generating capacity is specified as the annualized capital cost of a peaking unit allocated to peak hours. The annualized cost is $88,000/MW/year and this cost is allocated to 100 peak hours in the summer. The hot summer day that this study tested is assumed to have 2 peak hours, implying that the price of capacity is 2 x 88,000 / 100 = $1,760/MW. The final parts of Table 1.4 and Table 1.5 add in the savings in gasoline purchases by owners of PHEVs. The average driver is assumed to commute 27.2 miles in a vehicle that goes 20 miles per gallon using gasoline that costs $4/gallon. Compared to the Base Load in the high ramping cost case, the total system cost plus the savings in gasoline is 16.7% lower for Net Load and 30.4% lower for the Optimum Load. Similar cost reductions occur for the low ramping cost case. This reduction for Optimum Load are large and suggest that there are possibilities for reducing the total system cost of conventional generation and make the smart grid affordable to customers.

Table 1.6: Composition of Payments for energy and ramping per day by Conventional Demand(CD), Wind Generation(WG), Conventional Generation(CG), and Deferrable Demand(DD), low ramp cost case

	Ramping Payment ($1000)	Energy Payment ($1000)	Total Payment ($1000)	Total Energy (MWh)	Average Payment ($/MWh)
1) CD**	79	18,684	18,763	214,911	87
2) WG**	46	-2,129	-2,083	27,070	-77
3) CG**	-47	-16,594	-16,640	196,924	-85
4) DD**	-78	39	-39	9,523	-4

* Positive (Negative) values indicate Paying (Being Paid) for a service.

**CD, Conventional Demand and DD, Deferrable Demand

**WG, Wind Generation and CG, Conventional Generation

Table 1.7: Composition of Payments for energy and ramping per day by Conventional Demand(CD), Wind Generation(WG), Conventional Generation(CG), and Deferrable Demand(DD), high ramp cost case

	Ramping Payment ($1000)	Energy Payment ($1000)	Total Payment ($1000)	Total Energy (MWh)	Average Payment ($/MWh)
1) CD**	1,432	18,717	20,149	214,911	94
2) WG**	901	-2,133	-1,231	27,070	-45
3) CG**	-778	-16,984	-17,761	196,005	-91
4) DD**	-1,556	399	-1,157	9,840	-118

* Positive (Negative) values indicate Paying (Being Paid) for a service.
**CD, Conventional Demand and DD, Deferrable Demand
**WG, Wind Generation and CG, Conventional Generation

Table 1.6 and Table 1.7 illustrate the composition of net payments for purchasing energy and ramping. Here, the ramping payment is the sum of the ramp reserve cost and ramp wear-and-tear cost, and it is positive when causing or demanding ramping and negative when offsetting or supplying ramping. Four types of market participants are specified: Conventional Demand (CD), Wind Generation (WG), Conventional Generation (CG), and Deferrable Demand (DD). In the ramping payment column, CD and WG buy ramping services because they cause ramping. CD creates the initial daily pattern of ramping and WG increases the daily ramping slightly and adds variability from hour to hour. CG and DD provide ramping services because they mitigate the ramping caused by CD and WG. However, the ramping supplied by CG also causes the real out-of-pocket costs of ramping. In contrast, the real cost of providing ramping by DD is due to the inefficiency of storage. For energy, CD and DD are energy buyers (PHEVs can also supply some energy), and WG and CG are

energy suppliers.

The high ramping cost case in Table 1.7 shows that WG accounts for 11% of the energy supply and 38% of the ramping demand, and DD accounts for 2% of the energy demand and 67% of the ramping supply. These results illustrate that even though WG and DD are small components of the total energy payment, they are key components for causing and mitigating ramping. Allocating the total cost plus payment to the amount of energy purchased or generated shows that the net price of energy paid by CD is \$94/MWh and the price paid to CG is \$91/MWh. However, the price paid to WG is only \$45/MWh because WG has to pay for ramping. In contrast, DD is paid \$118/MWh because the value of supplying ramping is so much higher than the cost of buying energy. In the low ramping cost case in Table 1.6, the price paid to WG is higher, \$77/MWh, and the price paid to DD is much lower, \$4/MWh. This demonstrates that the level of the ramping cost determines the system cost of the variability associated with WG and the value of mitigating the ramping caused by WG and CD.

It should be noted that these results in Table 1.6 and Table 1.7 are illustrative and they would be more difficult to implement on a real network because of the different locations of load and generation. However, the important conclusion from this section is that combining WG and DD leads to much lower total system costs compared to a traditional system with no storage, and this conclusion does hold for this analyses using a network. The next step for future research is to determine whether these savings in the system cost with WG and DD are big enough to cover the capital cost of investing in wind capacity and storage.

Finally, Figure 1.3 illustrates how the composition of air conditioning and thermal storage changes to meet the hourly demand for cooling in the high

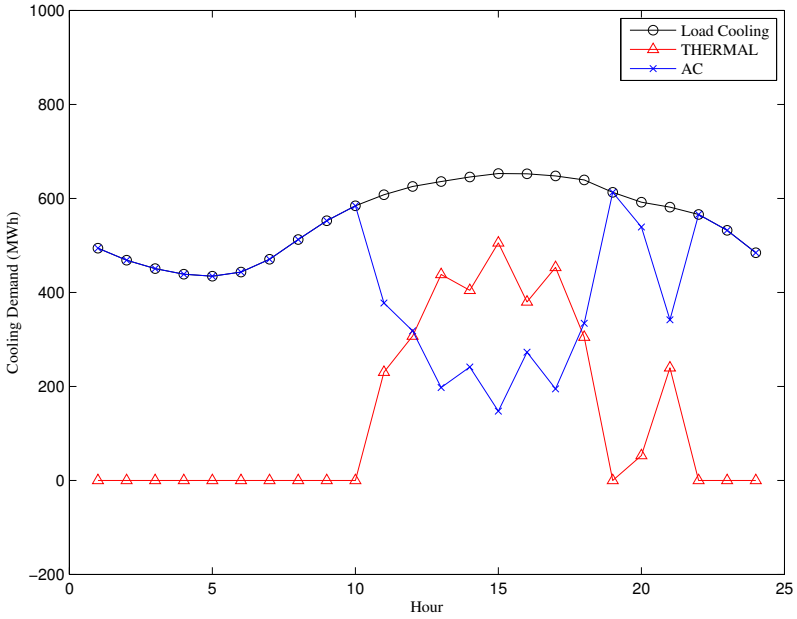

Figure 1.3: Daily Composition of Cooling Load : Direct cooling from air conditioner vs. Stored cooling from Thermal storage, high ramping cost case

ramping cost case. It shows that thermal storage shifts load from peak to off-peak hours and also provides a significant ramping service.

In this section, I compared the system results of two different ramping cost cases. The most important impact of high ramping costs on the system is that wind generation becomes less attractive because it adds significant stress to the conventional generation in terms of wear-and-tear cost, and deferrable demand is more valuable because it is an effective way to mitigate this ramping cost. According to Lefton et al. (2006), ramping-related costs are significantly under-estimated by industry and the ranges of actual ramping costs are high. Also as mentioned earlier, Troy (2011) showed that including the ramping cost in the optimization reduces the actual system cost by approximately 14%. The reduction in system cost that I observed for the high ramping cost case in Table 1.5

is only 10%. Therefore, I believe that the high ramp wear-and-tear coefficient specified in the high ramping cost case is more realistic for determining the impact of the ramping cost on the power system than the low ramp wear-and-tear coefficient. For this reason, I will show the results for the high ramping cost case only in the following analysis of costs for different types of customers.

1.3.2 Total Payments by Different Types of Customers

To compute the total bill for different types of customers, this study assumes initially that there are one million customers with identical daily patterns of demand. The following four different types of customer are identified: 1) customers who own no storage, 2) customers who add thermal storage, 3) customers who buy a PHEV, and 4) customers who own both thermal storage and a PHEV. These customers pay for three services that the electricity market provides. They pay for 1) energy using real-time pricing, 2) capacity using a demand charge based on their purchase of energy at the peak system load, and 3) reserve using the real-time marginal cost of ramp wear-and-tear and the fixed cost/MW of ramp reserve and operating reserve. For both energy and reserve, they can also be paid for by supplying these services.

Table 1.8 summarizes the total payment for each type of customer for the Optimum Load as well as for the typical customer for the Base Load and Net Load. The analysis of the Total System Costs in Table 1.5 shows that reductions in the reserve payment and capacity payment are important for customers with storage. This conclusion is reinforced in Table 1.8. A customer with thermal storage, in particular, makes a major contribution to reducing the ramping and capacity

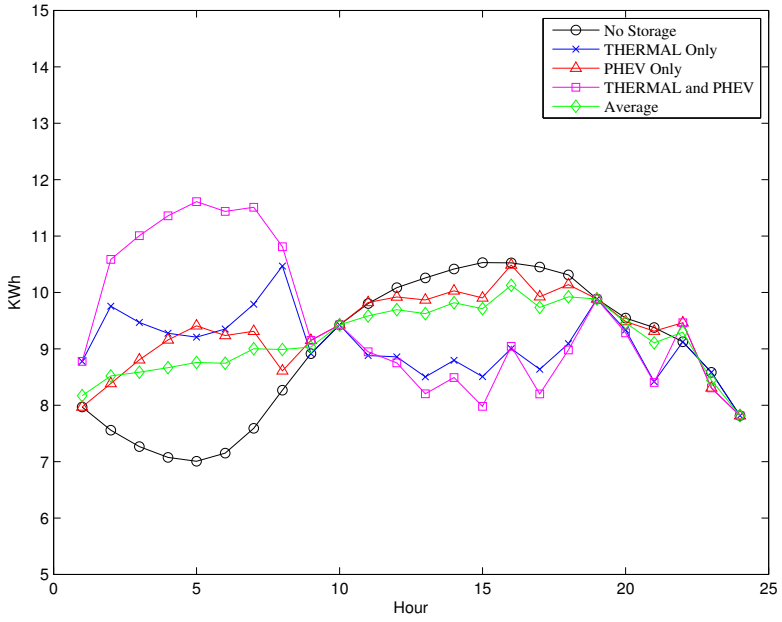

Figure 1.4: Daily Energy Demand by Four Types of Customers : Customers with no storage, thermal storage only, PHEV only, and both thermal storage and PHEV

cost by \$0.81/day and \$3.91/day, respectively, compared to a customer with no storage, whereas the corresponding reductions for customers with a PHEV are only \$0.38/day and \$1.21/day, respectively. This outcome is also evident in Figure 1.4. Customers with thermal storage are doing the heavy lifting by increasing demand in the early morning and reducing demand in the afternoon peak hours. The reason that thermal storage is more effective than PHEVs in trimming the peak conventional generation and mitigating ramping is because much of the stored energy in PHEVs is needed for commuting. In this sense, thermal storage is a more efficient form of deferrable demand for the grid. Although more total energy is purchased to charge a PHEV, this cost is offset by paying less to buy gasoline. Taking this into account implies that the net payment of energy is reduced by 16.6% and 13.0% for a PHEV owner and a thermal

Table 1.8: Total Payments by Four Types of Customers per day, high ramping cost case

	Base Load	Net Load	No Storage	THERMAL only	PHEV only	THERMAL & PHEV	Average
Energy Payment ($)*	24.48	18.03	18.72	18.24	19.11	18.70	18.79
Reserve Payment ($)**	1.58	1.66	0.91	0.10	0.53	-0.26	0.52
Total Payment ($)	26.06	19.69	19.63	18.34	19.64	18.44	19.31
kW at System Peak (kW)	11.58	11.58	11.58	9.36	10.89	8.78	10.68
Capacity Payment ($)	20.38	20.38	20.38	16.47	19.17	15.45	18.80
Total System Payment ($)	46.44	40.07	40.01	34.81	38.81	33.89	38.11
Savings in Gasoline ($)	0	0	0	0	5.44	5.44	2.72
Average Payment ($)	46.44	40.07	40.01	34.81	33.37	28.45	35.390
% Reduction from Base Load		13.7%	13.8%	25.1%	28.1%	38.7%	23.8%
% Reduction from No Storage				13.0%	16.6%	28.9%	11.6%

* Energy Payment Includes the Value of FEIS.

storage owner, respectively, compared to having no storage. The corresponding reduction for a customer with both thermal storage and a PHEV of 28.9% is by far the largest. Although the energy payments are similar for all four types of customers due to the flattening of the daily load profile, customers with deferrable demand benefit from lower payments for ramping and capacity.

Table 1.9 compares the total payments per customer using the optimum price payment with a flat regulated price for energy that includes all costs. The flat price is similar to the rate structures paid by many retail customers, and it is calculated by aggregating all system costs, including energy, ramping, and capacity, and dividing this total by the total amount of energy purchased in the market. This ensures that the same total payment is received from both pricing schemes. In contrast to the optimum price payment which shows substantial reductions for customers with storage, the flat price payment shows that cus-

Table 1.9: Total Payments Per Customers Using a Flat Regulated Price for Energy per day

	No Storage	Thermal Only	PHEV only	Thermal & PHEV	Average
Energy Purchased (KWh)	214.9	217.9	223.8	227.4	220.1
saving in Gasoline ($)	-	-	5.44	5.44	2.72
Optimum Price Payment ($)*	40.01	34.81	38.81	33.89	38.11
% Change from Average (%)	5.0%	-8.7%	1.8%	-11.1%	-
Flat Price Payment ($)*	37.21	37.72	38.75	39.38	38.11
% Change from Average (%)	-2.4%	-1.0%	1.7%	3.3%	-

* Gasoline Cost Saving is excluded.

** The Flat Price Payments are all scaled so that the average payment is the same as the average Optimum Payment.

tomers who own both thermal storage and a PHEV actually pay 3.3% more than the average customer, and customers with no storage pay 2.4% less. In other words, the flat price payment provides perverse economic incentives and the free riders with no storage are the winners. The main reason why the customers with both storage pay more under the flat price payment is because they have higher energy purchases due to storage inefficiency and the energy needed for commuting. Existing retail rate structures will have to be substantially modified to reflect the true costs incurred by a customer before customers or aggregators will be persuaded to participate more actively in the wholesale market. Real-time pricing for energy is a necessary but not sufficient step for expanding the role of deferrable demand in the smart grid. [4]

[4]It should be noted that some customers may choose to pay an aggregator a flat price but these types of financial contracts will be influenced by prices in the real-time wholesale market

1.3.3 Payback Periods

The objective of Figure 1.5 is to determine the payback periods for investing in different deferrable demand (DD) capabilities under the two pricing systems considered in Table 1.9: optimum prices and flat prices. Figure 1.5 shows the cumulative annual incremental costs of purchasing electricity over 15 years for the three types of DD customers relative to a customer with no DD storage using a 0% and a 4% discount rate. The DD customers own either thermal storage, a PHEV or both thermal storage and a PHEV, and the flat rates are specified to raise the same amount of daily revenue as the optimum rates. The daily cost of purchasing electricity for a customer with no DD storage is subtracted from the corresponding cost for each type of DD customer to give an incremental cost savings. To determine the annual costs, optimizations for four different daily load patterns, representing the four different seasons, were computed. Other inputs and prices were kept constant in the different seasons and different years. Aggregating the increments over the four seasons gives an estimate of the annual savings in the cost of meeting energy needs for the three types of DD customers. [5]

Customers who do not own a PHEV are assumed to have a conventional gasoline vehicle (CV), and customers with no thermal storage are assumed to have a conventional AC unit. Consequently, the higher cost of purchasing a PHEV and/or the cost of installing thermal storage should be taken into account

[5]It should be noted that the incremental cost of capital in the optimal rate is only non-zero in the summer because this cost represents a reduction in the installed conventional capacity needed to meet the peak system load. The full capital cost of a peaking unit is covered by the demand charge in the summer months even though, in practice, payments would be spread out in some way throughout the year.

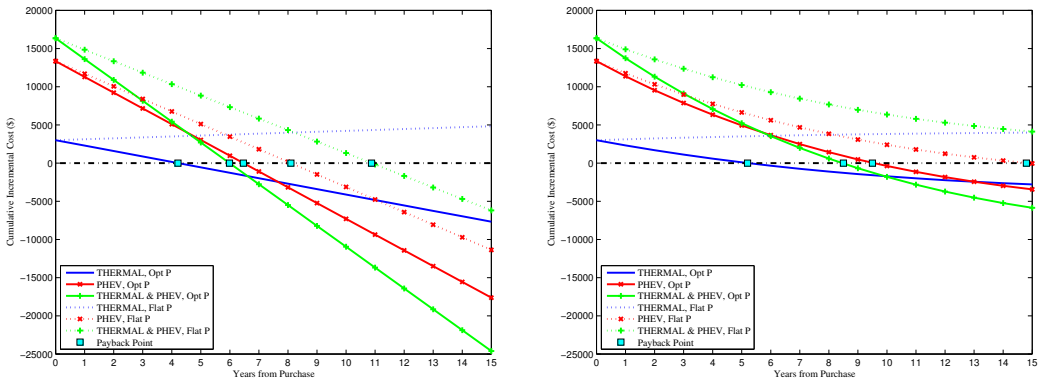

(a) without the discount rate (b) with the discount rate, 4%

Figure 1.5: Cumulative Incremental Annual Costs for Customers with DD capabilities relative to Customers with no DD storage using Optimum Prices and Flat Prices

to estimate the full incremental cost for a customer with DD capabilities. For a PHEV, the additional cost corresponds to purchasing a GM Volt instead of a CV of an equivalent size, and it is equal to \$12,496.[6] In addition to this cost, the cost of a smart charger, \$849, is also included because this is essential for managing charging.[7] Hence, the total additional cost of buying a PHEV is \$13,345.

Using the same specifications as Table 1.5, the gasoline price is \$4/gallon in NYC, the fuel efficiency is 20 miles/gallon, and the daily average driving distance is 27.7 miles. Consequently, the savings in the cost of gasoline for a customer who owns a PHEV is \$5.44/day.

There is less available information about the capital cost of thermal storage. A paper by MacCracken (2010) gives the range of cost from \$30/kWh to \$150/kWh for energy capacity. The reason for this large range is that adding

[6]The cost of a Volt, based on market data from GM, is \$32,495 (\$39,995 (MSRP) - \$7,500 (tax benefit)), and the cost of a CV is \$19,999.

[7]GE WattStation, Level 2 charger with a charging rate up to 7.2 kW

thermal storage to a building cooling system has implications for the existing AC equipment. Capital cost reductions can often be achieved by downsizing other cooling equipment. To avoid overestimating the benefits of thermal storage, I chose the high cost of \$150/kWh, and the cost of installing thermal storage is \$3,000 for the 20kWh unit specified for a customer with thermal storage. In spite of specifying a high capital cost for installing thermal storage, it is less than a quarter of the incremental cost of purchasing a PHEV.

In Figure 1.5, the initial investment in DD capabilities is made at time zero, and when the cost line is above zero, the cumulative savings have not paid back the initial investment. The year when a line crosses the x-axis is the payback period for the investment. When the optimum prices are used, the payback periods for customers with thermal storage, a PHEV and both thermal storage and a PHEV are 4.2 years, 6.5 years and 6 years, respectively, if there is no discounting. Considering that the average life of a battery for a PHEV is 7 to 8 years, the payback periods for customers with a PHEV are short enough to justify the investment. The replacement time for thermal storage is likely to be even longer, and as a result, the investments in DD capabilities are economically viable for all three types of customers if the optimum prices are paid.

The results for customers paying flat prices are completely different. Having thermal storage increases annual costs for the same amount of cooling delivered because of the physical inefficiencies of the storage. Although the saving in gasoline purchased for a PHEV owner is enough to cover the cost of charging the battery, the payback period for a PHEV customer is now slightly longer than the life of the battery, 8.1 years. Things are even worse for a PHEV customer with thermal storage because the payback period is 10.9 years, roughly twice as

long as it is using the optimum prices.

If this study considers the 4% discount rate as shown in Figure 1.5(b), the payback periods for customers with thermal storage, a PHEV and both thermal storage and a PHEV are 5.2 years, 9.5 years and 8.5 years under optimum prices, respectively, and the payback periods under flat prices are much longer so that storage is never economically viable. This example clearly shows that the optimum prices provide the proper incentives for purchasing a PHEV and/or thermal storage, whereas flat prices reduce the incentives for purchasing a PHEV and are perverse for thermal storage.

1.3.4 Diminishing Marginal Reduction in System Costs

Figure 1.6 illustrates the total system cost with different amounts of thermal storage for the Optimum Load with wind generation but no PHEVs. The thermal storage in Figure 1.6 ranges from 0 GWh (i.e. Net Load) to 10 GWh (twice the capacity specified in the previous analysis). The results exhibit diminishing marginal reductions in the total system cost, and when the storage reaches 10 GWh, the marginal cost reduction is trivially small. Once the net load profile is flattened and smoothed by the storage, no more cost reductions are possible. Additional storage would be left idle.

1.4 Discussion and Conclusions

The adverse environmental effects of emissions from fossil power plants and vehicles have led to an increase in the use of various types of renewable energy

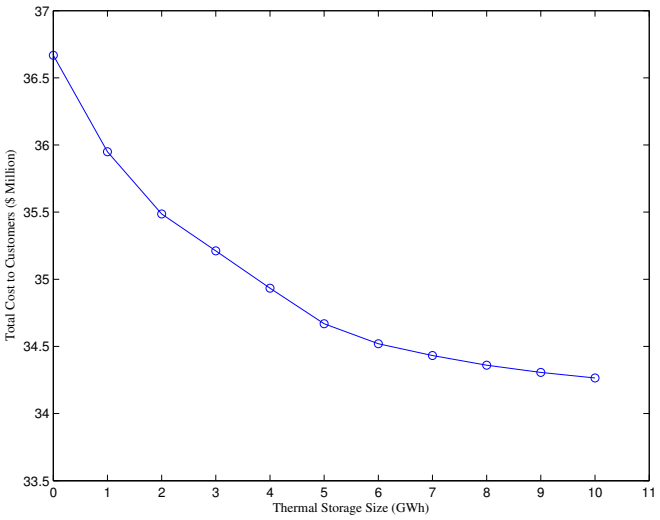

Figure 1.6: Total Cost to Customers with various sizes of thermal storage

for generating electricity. Due to the non-dispatchable characteristics of these renewable sources, there are major benefits from using storage to mitigate the inherent variability of renewable generation. Deferrable demand, that decouples the purchase of electricity from the delivery of an energy service, provides a relatively inexpensive form of storage compared to dedicated utility-scale storage. Although the smart charging of PHEVs is a well-known type of deferrable demand, the relatively small size of the total storage capacity of PHEV batteries limits its effectiveness. From the perspective of the electric delivery system, a PHEV is an inefficient battery because a significant amount of the electricity stored is used for transportation. In contrast, thermal storage for space cooling is relatively efficient and has a much larger potential capacity.

This chapter investigates how thermal storage and PHEVs can help to lower the total system cost of supplying electricity and customers' bills in an electricity market with a high penetration of wind generation. The data represent the hourly demand for electricity on a hot summer day in New York City and dis-

tinguish between Temperature Sensitive Demand (TSD), which can potentially be converted to thermal storage, and Non-Temperature Sensitive Demand (N-TSD), such as lighting. An economic model of electricity supply is developed to minimize the total daily cost of the energy and ramping associated using conventional generating units. Wind generation is treated as a free exogenous input, and there is no cost from using storage other than the inherent inefficiency of this capacity. The specified storage capacities for energy in New York City are 5 GWh for thermal storage (corresponding to 6.2% of the TSD) and 5 GWh for PHEVs (corresponding to 44.2% of the number of commuting vehicles). The big difference in these two percentages illustrates why the potential capacity of thermal storage is so much larger than the capacity of PHEV batteries.

Comparing the total supply costs for different scenarios, including the capital cost of the conventional generating units and the savings in gasoline purchases from PHEVs, this studyfound that adding wind generation reduces the total daily supply cost (in the high ramp cost case) by 17%, and adding thermal storage and PHEVs reduces the total cost by an additional 13% for a total of 30%. This significant cost reduction of 30% comes from lowering energy, reserve and capacity costs by $3.6 million (35%), $0.5 million (58%), and $2.8 million (14%) per day, respectively. In addition, savings in gasoline purchases accounts for an additional $2.7 million. Even though the largest percentage reduction in costs is for reserve capacity, this reduction is by far the smallest compared to the other reductions.

Since the displacement of fossil fuels by wind generation is largely responsible for the lower energy costs, the most important reductions in costs associated with deferrable demand are from lower capacity costs (due to moving

demand from peak to off-peak periods), and from purchasing less gasoline. In fact, adding deferrable demand actually increases the energy cost, compared to the case with wind generation, because 1) charging the PHEV batteries represents a new source of demand, and 2) there are inevitable inefficiencies in the charge/discharge cycles for both PHEVs and thermal storage. To get a better understanding of the demand and supply of energy and reserves (ramping), this study categorizes Conventional Demand (CD) and Deferrable Demand (DD) as the buyers of energy and Conventional Generation (CG) and Wind Generation (WG) as the suppliers of energy. In contrast, CD and WG are the buyers of ramping services, since they create the need for ramping, and DD and CG are the suppliers of ramping services. (Note that by providing ramping services, CG also incurs additional out-of-pocket expenses.) The results indicate that WG accounts for 11% of energy supply and 38% of ramping demand, and DD accounts for 2% of energy demand and 67% of ramping supply. Even though WG and DD are minor players in the market for energy, they are the key players in the market for ramping.

In the analysis of payments by different types of customers, the net cost paid by a typical customer with thermal storage only, with a PHEV only, and with both a PHEV and thermal storage is 13.0%, 16.6%, and 28.9% lower, respectively, than the cost for a customer with no storage capabilities. However, customers with no storage and with thermal storage only have exactly the same daily profile of energy services delivered (CD plus the demand for cooling) and customers with a PHEV use more energy. A customer with both a PHEV and thermal storage achieves the biggest savings. Since DD reduces the price difference between peak and off-peak periods by flattening the daily purchases of electricity, the main savings come from lower ramping costs and lower capi-

tal costs. However, realizing these savings for customers would require that all customers 1) are exposed to the real-time price for the electric energy purchased, 2) pay a demand charge for their actual purchase of electricity at the peak system load, and 3) pay for the ramping services used or are paid for the ramping services provided.

The main conclusion is that regulatory changes will be needed to ensure that customers with DD capabilities pay rates that reflect their true net-cost to the grid and provide the financial incentives for investing in the DD capabilities needed to realize the cost savings described in this chapter. To illustrate this conclusion, this study shows that the standard regulatory practice of charging a flat retail price for energy, in effect, subsidizes customers with no storage and penalizes customers with DD. Although managing DD and selling ramping services require substantial knowledge of how power systems operate, this study assumes implicitly that the grid will have a hierarchical structure and that aggregators will manage the DD appliances of individual customers. The incentive for customers with DD is that their electric bills will be lower and they will still get the same energy services delivered when they need them. The system operator will provide each aggregator with market signals and will treat the combined demand from individual customers as a single wholesale customer for billing purposes.

Each aggregator would pay real-time prices for the energy and ramping services purchased, and a demand charge for their use of capacity at the system peak. In addition, if an aggregator can reduce (increase) demand when up-ramping (down-ramping) is needed on the system, this aggregator would also be paid for providing ramping services. The financial objective of an aggrega-

tor would be to minimize their net payments to the System Operator, subject to meeting their customer's energy needs. These payments could then be prorated to determine the bills for individual customers if DD is metered separately from CD. In practice, there could be a number of different types of contracts for customers, and some customers might prefer to have traditional fixed-rate contracts. Nevertheless, customers who allow an aggregator to manage their DD should see direct benefits by paying lower bills. In summary, this study concludes that in order to build the foundation for a smart grid that customers can afford, the regulatory environment must change. The goal should be to develop a functioning two-sided market in which all participants in the various markets for electricity and ancillary services, including customers, pay for the services they use and are paid for the services they provide.

CHAPTER 2

CHARACTERISTICS OF WIND FARM, ELECTRICITY DEMAND, TEMPERATURE AND TECHNICAL SPECIFICATIONS OF DEFERRABLE DEMANDS AND UTILITY-SCALE STORAGE

2.1 Introduction

Wind generation has been accepted as a major renewable energy option in many states in the US and around the world in recent years. As the penetration of wind generation rapidly increases, the importance of accurately modeling and forecasting wind generation also increases. However, the high variability and uncertainty of wind makes it difficult to develop a model that can show the satisfying level of forecasting accuracy. Having a good model for wind and also for electricity demand is an important step to estimate the potential benefit of wind generation in the power system and the economic value of various types of energy storage systems (ESS) when they are combined with wind generation.

In this chapter, I analyze 1) how hundreds of wind sites and electricity demand regions in the New York State and New England areas are grouped and represented by fewer locations that demonstrate all important characteristics using principle component analysis, 2) how correlations among wind, electricity demand and temperature in selected sites look 3) how the modeling for wind and electricity demand is done and how these models are generating simulated profiles, 4) how wind speed is converted to wind power using a multi-turbine modeling approach by Norgaard and Hottlinen (2004), and 5) how the scenario realizations of wind power and electricity demand are generated so that they can be tested and run in the finite time using the Multi-Period Security Con-

strained Optimal Power Flow (SCOPF), the power system simulation platform developed at Cornell University (the second generation SuperOPF). I also show 6) the technical specifications of different types of energy storage systems which can improve the efficiency of wind generation by mitigating its high variability.

2.2 Processing Wind and Electricity Demand

Wind speed data used in this study are from the Eastern Wind and Transmission Study(EWITS) by the National Renewable Energy Laboratory(NREL). These data are simulated every 10 minutes and measured at 80m height from 2004 to 2006. These wind data are simulated at 179 sites, 66 sites from New York and 113 sites from New England area, and in each site, the dataset has 157,868 observations marked from 00:10 January 1, 2004 to 00:00 January 2, 2007. All sites are onshore sites. There is a separate dataset from NREL which contains information like potential MW capacity and average wind speed for each site. This information is used when potential MW capacity of each group is computed. Hourly day-ahead electricity demand data of New York state and New England regions are collected from the NYISO and NE-ISO website (www.nyiso.com and www.ne-iso.com).

Figure 2.1 is a one-line diagram of the 36-bus test network used in this study. This network is a New York and New England reduction of the Northeast Power Coordinating Council (NPCC) from Allen et al. (2008), and at each bus level, it is modified to include detailed information of the generating units from the PowerWorld Corporation. In this section, wind and electricity demand data are processed to match the raw data from NREL and two ISOs to available nodes

on the 36-bus test network. This test network completed with matched wind and electricity demand data is analyzed in Chapter 3.

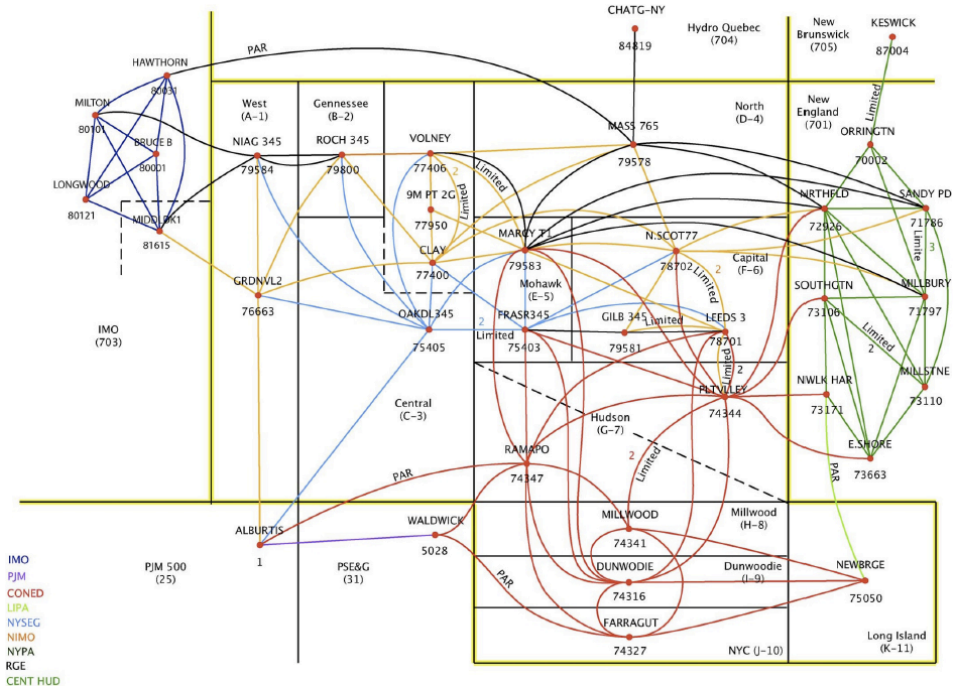

Figure 2.1: A One-Line-Diagram of the 36-Bus Test Network, Source: Allen et al. (2008)

2.2.1 Grouping Wind Sites and Electricity Demand Regions

Figure 2.2 shows the daily wind speed profile of all 179 sites from the data of January 1, 2004. It is notable in these plots that the wind profile patterns are largely different between New York (NY) and New England (NE) on this day, but within each region, there are strong patterns among variable profiles. For instance, NY shows thick clusters of profiles that stay close to each other and move in a decreasing direction, and NE shows less clear patterns but there exists a cluster that mostly stays in the middle with a little bump in early afternoon hours. This would mean that among the 179 sites of wind data in NY and NE,

there are sites that have similar statistical characteristics. Hence, I performed Principle Component Analysis (PCA) to capture different characteristics in different wind sites and group sites that show similar patterns.

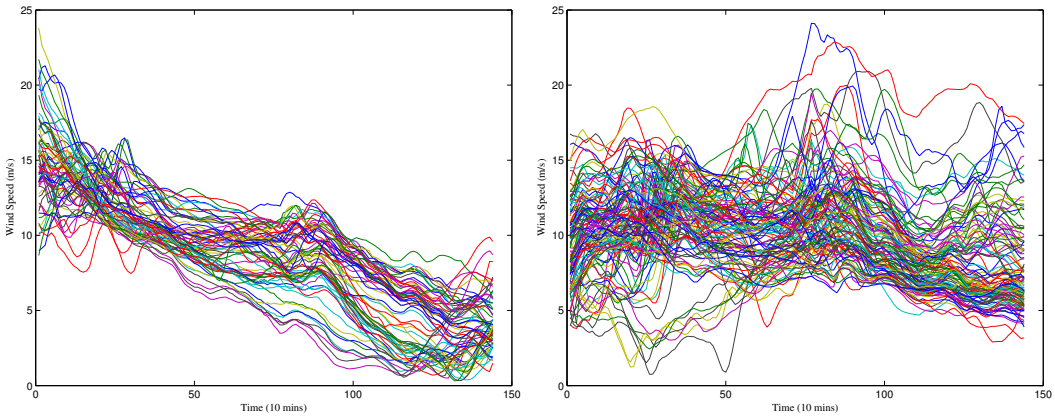

(a) New York, 66 sites (b) New England, 113 sites

Figure 2.2: Daily Profiles of Wind Speed for all 179 sites on 01-01-2004

Grouping Wind Sites

a) New York

Table 2.1 summarizes the results of PCA for NY. Each row in the table indicates the dimension of PCA that explains certain variances of dataset, and the 'Proportion' column shows how much variance of the total data is explained by the corresponding dimension. 'Cumulative' column shows the percentage of total variance explained up to the dimension. I made the cutoff point at 90% of the cumulative proportion and considered up to PCA9 for grouping.

Figure 2.3 shows the distributions of individual wind sites for each principle component dimension. The PCA 1 is not included here because it includes most of the sites and does not give any information for grouping. From PCA 2, PCA

Table 2.1: Definition of Variables, simplified Formulation

Dimension	Eigenvalue	Difference	Proportion	Cumulative
1	471.32	386.15	0.65	0.65
2	85.17	60.55	0.12	0.77
3	24.62	7.01	0.03	0.80
4	17.61	3.37	0.02	0.83
5	14.23	1.36	0.02	0.85
6	12.88	2.28	0.02	0.86
7	10.60	1.87	0.01	0.88
8	8.73	1.90	0.01	0.89
9	6.83	0.88	0.01	0.90

dimensions show a clear cluster of wind sites which helps grouping wind sites with similar characteristics. For instance, there are clear clusters of wind sites near Niagara, eastern NY, and northern NY in PCA 2 and PCA 3, which means that there are significant correlations among those sites. PCA 6 also says there are high correlations among sites in central NY .

Based on this PCA result and geographical characteristics, I grouped 66 wind sites of New York state into 9 locations. Table 2.2 shows which PCAs are considered to form each group, and the wind site that represents each group and the wind capacity of each group based on NREL dataset. The matching node of each wind group in the 36-bus test network is also specified. The four-digit number in the Representative Wind Site is site indexing number from the NREL dataset, and these representative wind sites selected for each group are sites that show the highest wind capacity. The Wind Capacity of each group is determined by aggregating the wind capacities of all sites in that group. These representative Wind Sites for each group will be located in the noted matching node in the network and analyzed in Chapter 3.

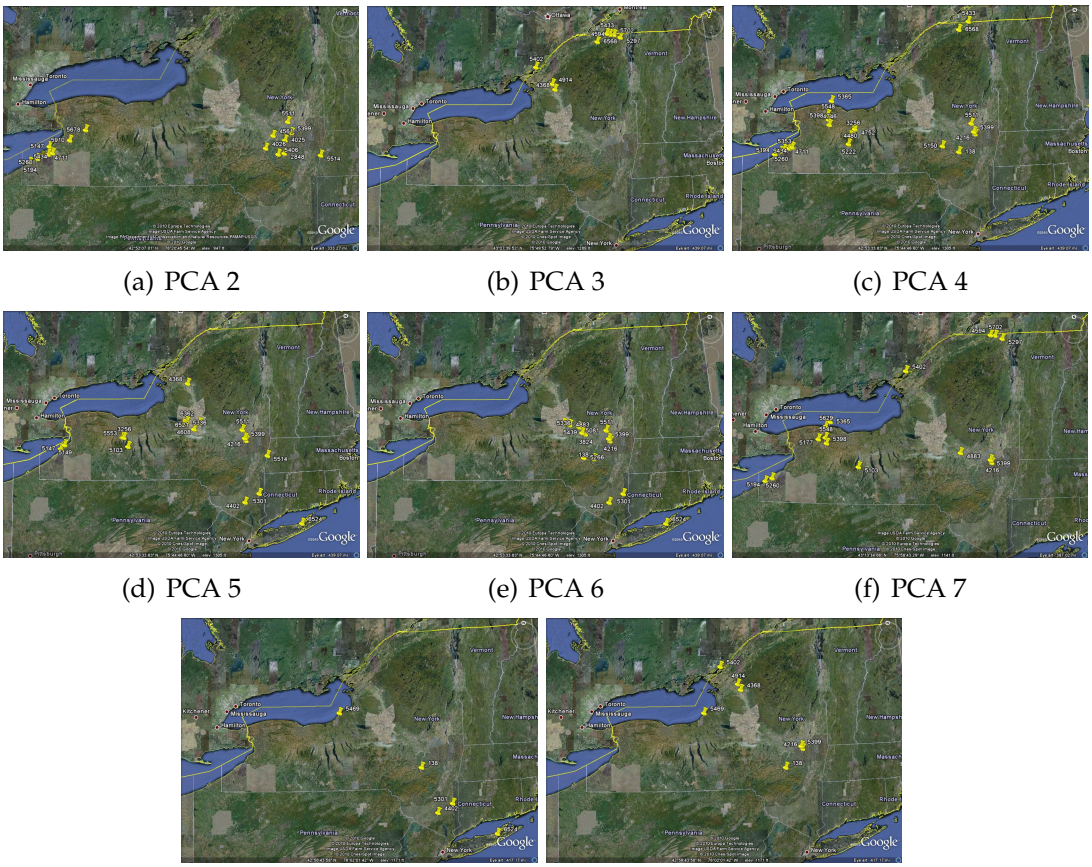

(a) PCA 2 (b) PCA 3 (c) PCA 4

(d) PCA 5 (e) PCA 6 (f) PCA 7

(g) PCA 8 (h) PCA 9

Figure 2.3: New York Wind Sites according to PCA analysis

Figure 2.4 summarizes the distribution of all 66 wind sites in NY and nine groups that I determined based on the principle component analysis and geographical characteristics.

b) New England

The same methodology is applied in grouping 113 wind sites in New England regions. Based on the principle component analysis shown in Table 2.3, PCA dimensions up to PCA 15 are taken into consideration. PCA 1 is not considered as the same reason mentioned in the New York case. Finally, the 113

Table 2.2: NY Wind Grouping affected by PCA Results

	Principle Component	Representative Wind Site	Wind Capacity (MW)	Matching node in the network
Group 1	PCA 2	4711	3031.6	Niagara
Group 2	PCA 6	3906	3810.5	Rochester
Group 3	PCA 4	3256	1587	9 Mile Point
Group 4	PCA 3	4368	2476.7	Massena
Group 5	PCA 4	4608	1133.6	Marcy
Group 6	PCA 7	138	1407.4	Gilboa
Group 7	PCA 2	2848	1095.7	Leeds
Group 8	PCA 7	4402	199.3	Farragut
Group 9	PCA 7	6524	117.6	Newbridge

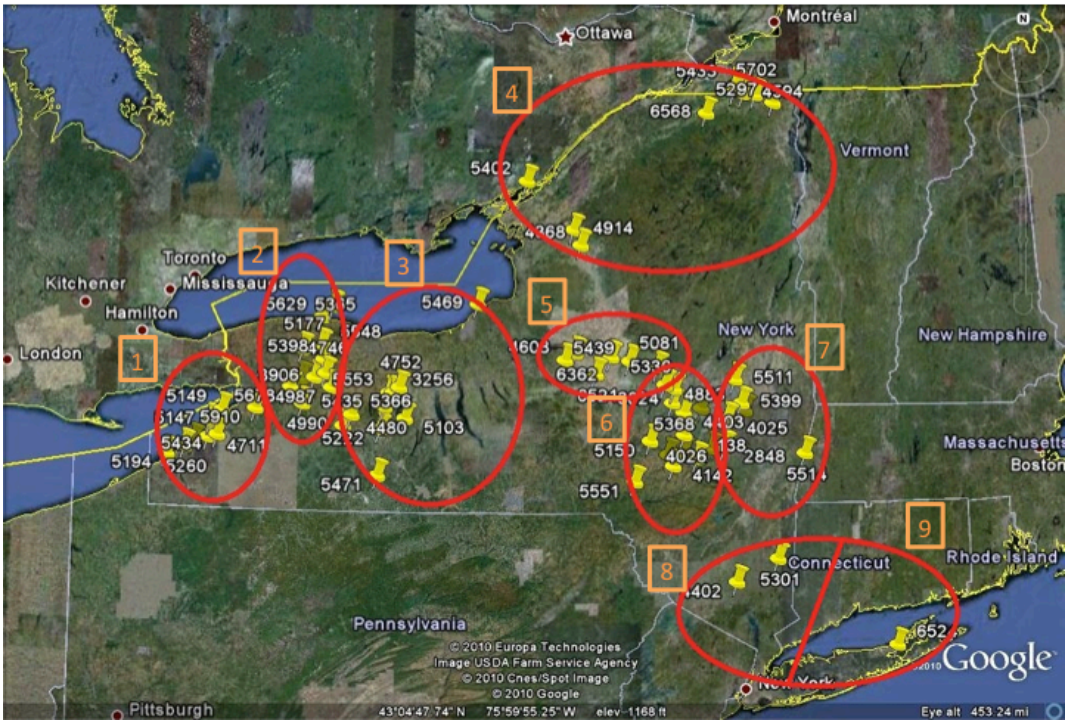

Figure 2.4: Locations of 9 Wind Groups in New Yprk

sites are grouped into 7 locations based on graphical representation of PCA dimensions upto PCA 15 in Figure 2.5 and geographical characteristics. Table 2.4 summarizes the 7 representative wind sites, their capacities and the matching

nodes in the test network. Figure 2.6 illustrates the distribution of all 113 wind sites and the locations of the 7 groups in the New England regions.

Table 2.3: Definition of Variables, simplified Formulation

	Eigenvalue	Difference	Proportion	Cumulative
1	778.45	661.03	0.631	0.631
2	117.41	58.25	0.095	0.727
3	59.16	22.35	0.048	0.774
4	36.81	11.27	0.030	0.804
5	25.54	6.65	0.021	0.825
6	18.89	6.03	0.015	0.840
7	12.86	1.34	0.010	0.851
8	11.51	1.26	0.009	0.860
9	10.26	2.36	0.008	0.868
10	7.90	0.08	0.006	0.875
11	7.82	0.65	0.006	0.881
12	7.17	0.74	0.006	0.887
13	6.43	0.35	0.005	0.892
14	6.07	0.06	0.005	0.897
15	6.01	1.08	0.005	0.902

Table 2.4: NE Wind Grouping affected by PCA Results

	Principle Component	Representative Wind Site	Wind Capacity (MW)	Matching node in the network
Group 1	PCA 2, PCA 6	1562	2634	Norwalk Harbor
Group 2	PCA 5	5549	1521.4	Millstone
Group 3	PCA 6, PCA 12	1945	1178.3	Southington
Group 4	PCA 7, PCA 10, PCA 11	3985	1605.1	Millbury
Group 5	PCA 3	196	2219.4	Northfield
Group 6	PCA 8, PCA 9, PCA 13	6	3472.8	Sandy Pond
Group 7	PCA 4	3825	1775.6	Orrington

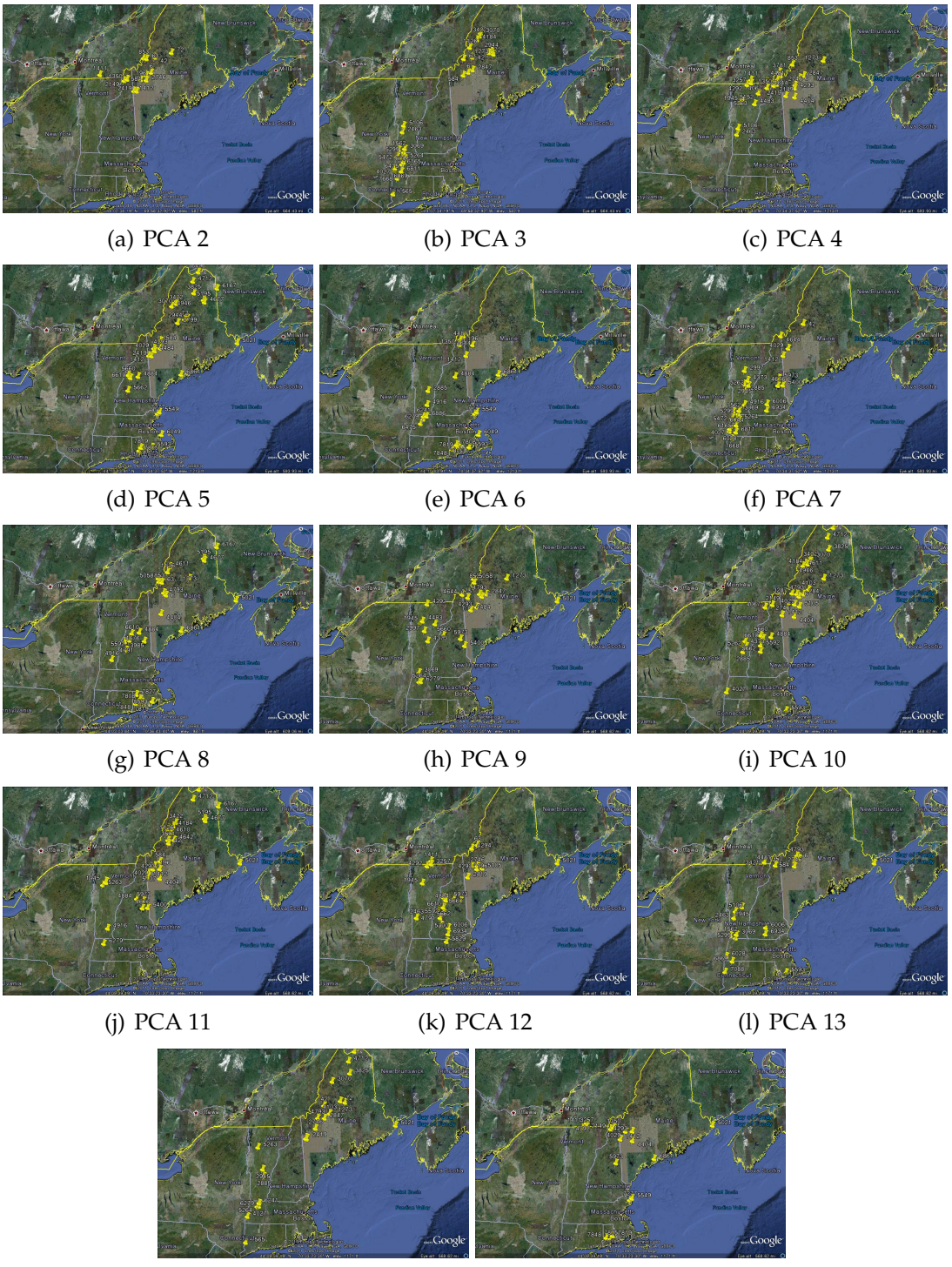

(a) PCA 2 (b) PCA 3 (c) PCA 4

(d) PCA 5 (e) PCA 6 (f) PCA 7

(g) PCA 8 (h) PCA 9 (i) PCA 10

(j) PCA 11 (k) PCA 12 (l) PCA 13

(m) PCA 14 (n) PCA 15

Figure 2.5: New England Wind Sites according to PCA analysis

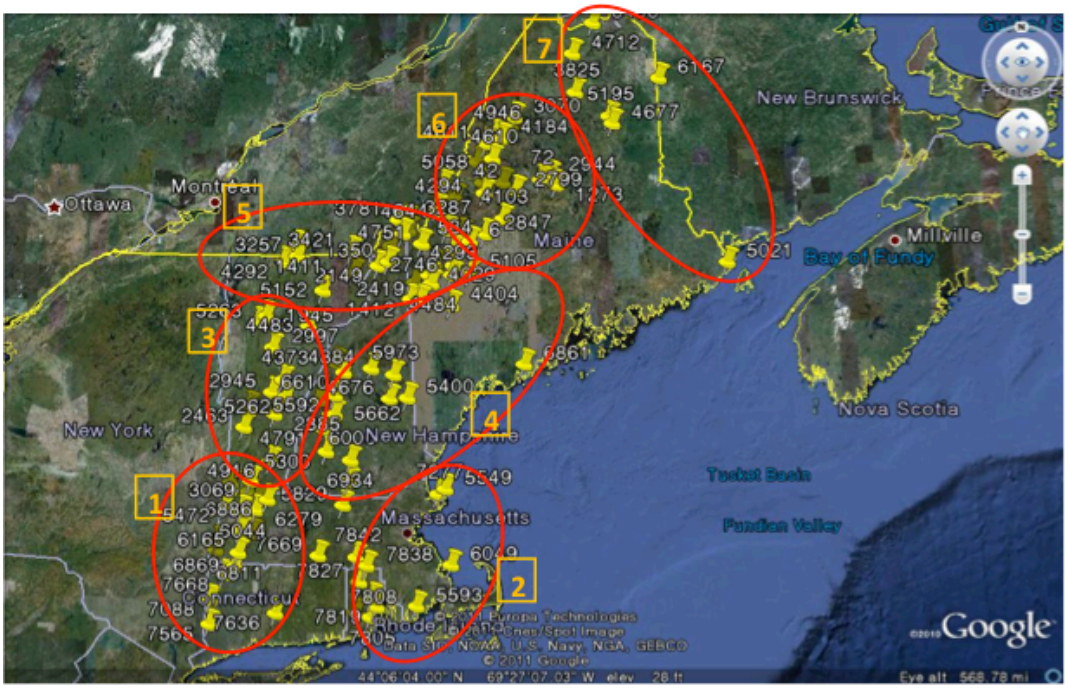

Figure 2.6: Locations of 7 Wind Groups in New England

Grouping Electricity Demand Regions

The ISO-NE classifies its area into 8 zones (Maine, New Hampshire, Vermont, Connecticut, Rhode Island, SE MASS, WC MASS, NE MASS Boston), and the NYISO classifies its area into 11 electricity demand zones (West, Genesee, Central, North, Mohawk Valley, Capital, Hudson Valley, Millwood, Dunwood, NYC and Long Island). The 8 New England zones are grouped into 3 regions (Northern NE, Southern NE and Boston), and the 11 New York zones are grouped into 4 regions (Western NY, Eastern NY, NYC and Long Island) using geographical characteristics. Figure 2.7 shows the locations of the 7 regions, and Table 2.5 summarizes the descriptions of each electricity demand region in New England and New York. These 7 regions will be matched to the test network map, and those nodes that belong to each regions will be applied to the region-specific

electricity demand information.

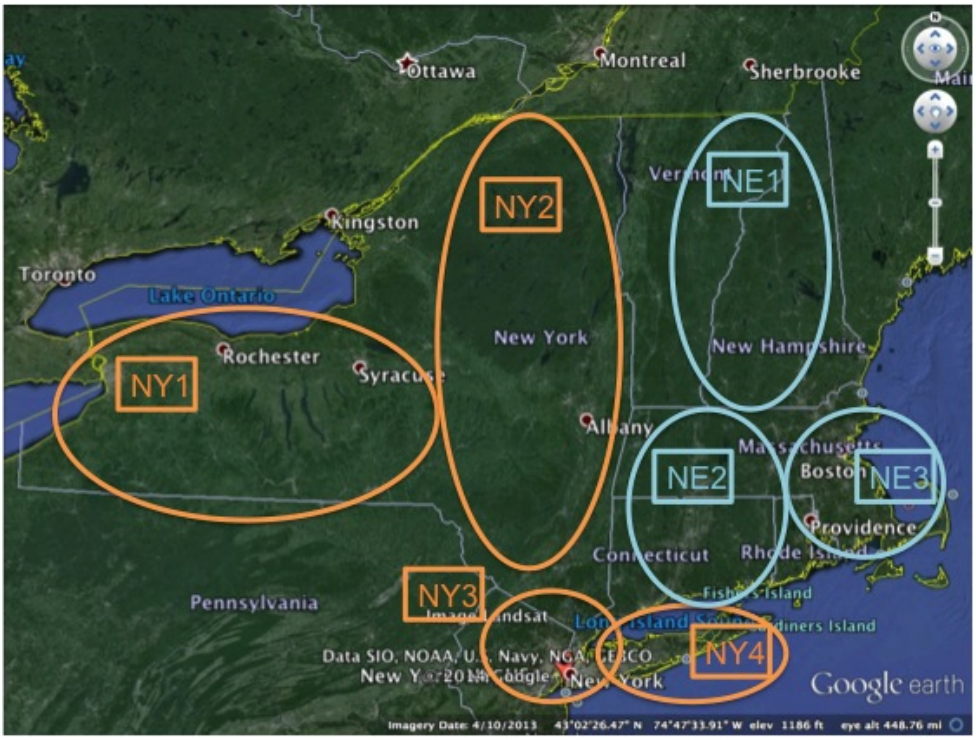

Figure 2.7: Locations of 7 Electricity Demand Regions in New York and New England

Table 2.5: Electricity Demand Regions in New York and New England

Regions	Group	Location
Region 1	NE1	Northern NE
Region 2	NE2	Southern NE
Region 3	NE3	Boston Area
Region 4	NY1	Western NY
Region 5	NY2	Eastern NY
Region 6	NY3	New York City
Region 7	NY4	Long Island

2.2.2 Correlations among Wind, Electricity Demand and Temperature

In this section, I investigate correlations among selected wind sites, electricity demand regions, and matching temperature information. Temperature data is from the Northeast Regional Climate Center(NRCC) at Cornell University. Their dataset is hourly and includes geographic information regarding latitude, longitude and elevation of points of measuring. The dataset includes temperature data from 34 sites in New York and 73 sites in New England. This correlation information is useful in understanding the variance and covariance relationship among and between each site and each dataset, and is helpful in developing better forecasting models of wind and electricity demand.

Correlations among Wind and Electricity Demand

Figure 2.8 illustrates the graphical representation of the correlations for 16 wind sites and 7 electricity demand regions. The first 7 wind sites (w1-w7) in this figure are the 7 selected wind sites in New England, and the latter 9 sites (w8-w16) are wind sites in New York. Demand regions (L1-L7) are in the order of regions stated in Table 2.5. When the color of a cell is close to red, the correlation is generally high and close to 1, and when the color is close to blue, correlation is close to 0. When the color is close to yellow, the correlation is moderate and close to 0.5. Correlations among the wind sites are relatively lower than correlations among the electricity demand regions as there are many yellow or green cells in correlations among wind sites. Correlations between wind and electricity demand are all very low close to 0. Among the wind sites, I see that when

wind sites have good proximity to each other, they show higher correlations like the wind sites in New England (w1-w7) that shows notably higher correlations. W13 located in central New York seems like an outlier.

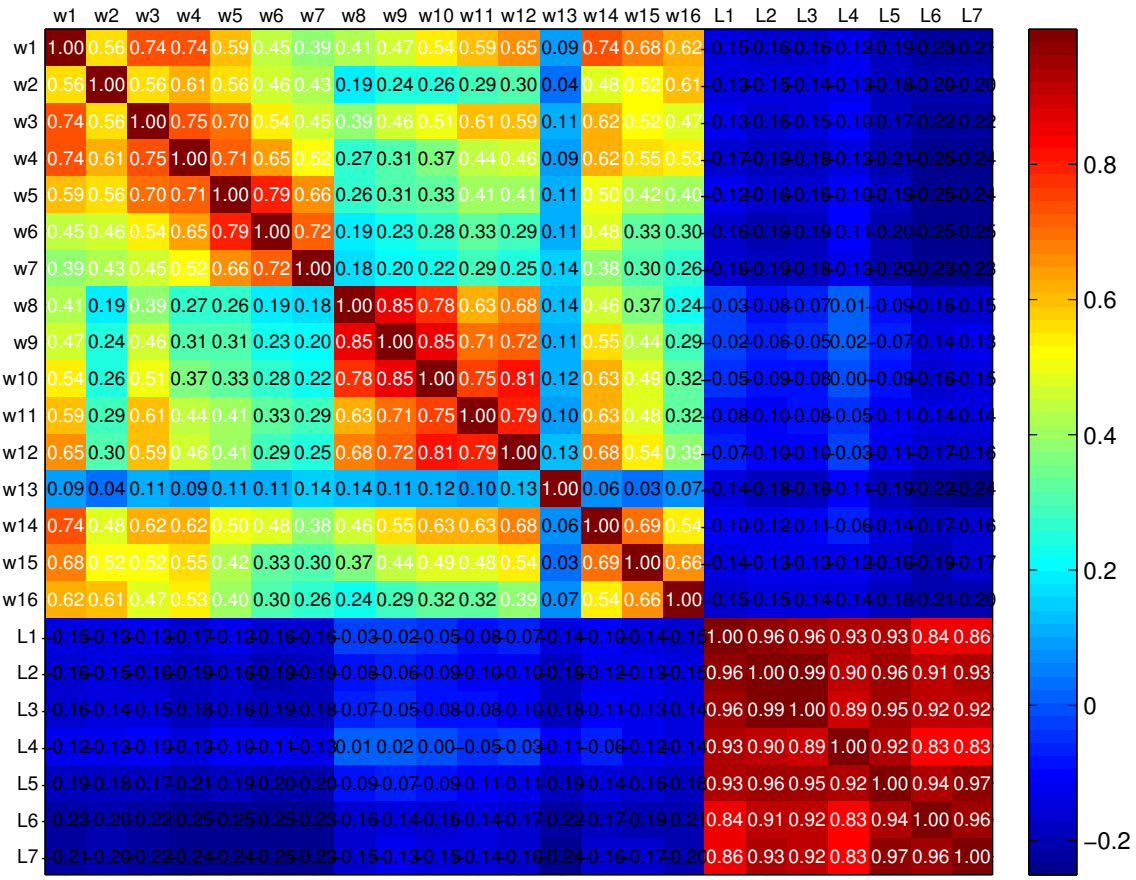

Figure 2.8: Correlations among Wind and Electricity Demand

Correlations among Wind and Temperature

Figure 2.9 illustrates the correlation among wind and temperature in New York and New England. In both areas, correlations among temperature are slightly higher than correlations among wind sites, but the difference is marginal. The

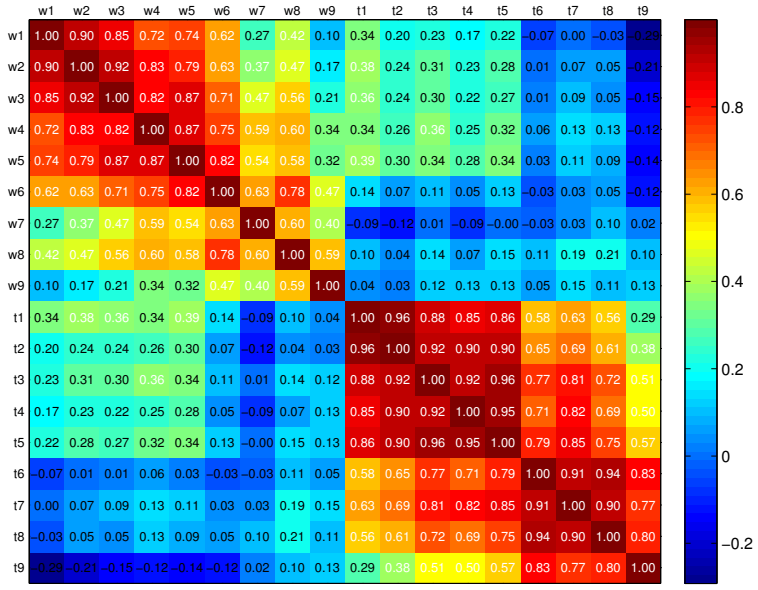

(a) New York

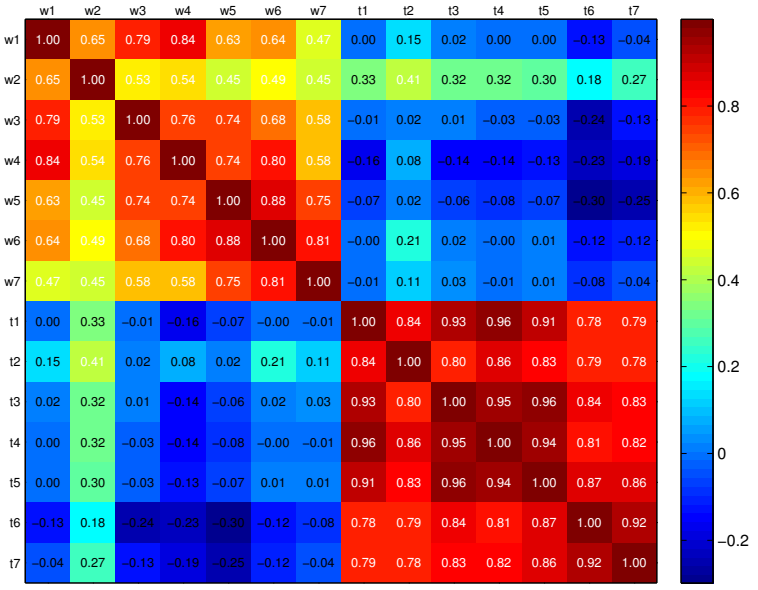

(b) New England

Figure 2.9: Correlations among Wind and Temperature

correlations between wind and temperature are fairly low from -0.1 to 0.3 and are mostly mostly blue shaded in both area. However, in certain regions in New York (w1-w5), the correlations between wind and temperature show some

meaningful values (0.2 to 0.35) as seen in the green shaded areas. This shows that correlations between wind and temperature are weak but have some low positive correlation.

Correlations among Electricity Demand and Temperature

Figure 2.10 gives a graphical representation of correlations among electricity demand and temperature in New York and New England. The relationship between electricity demand and temperature was mentioned in section 1.2.1 when I introduced the concept of Temperature-Sensitive Demand (TSD). Figure 2.10-(a) does not support the idea of TSD well, since the correlations between electricity demand and temperature are not very significant, but Figure 2.10-(a) shows correlations for the whole year when there are seasons whereTSD is not very high because TSD is mostly caused by the use of air conditioning on hot summer days. This idea of TSD is confirmed in Figure 2.10-(b), which shows correlations only in the summer season. As colors of cells between electricity demand and temperature indicate, the positive relationship is very strong between demand and temperature in summer season. Therefore, when modeling the electricity demand, temperature can be an important explanatory variable, and by taking out the deterministic part that is explained by temperature, TSD can be estimated.

2.2.3 Modeling Wind and Electricity Demand

The temperature and wind speed for 16 locations, and electricity demand for 7 locations in New York and New England regions are estimated by econometric

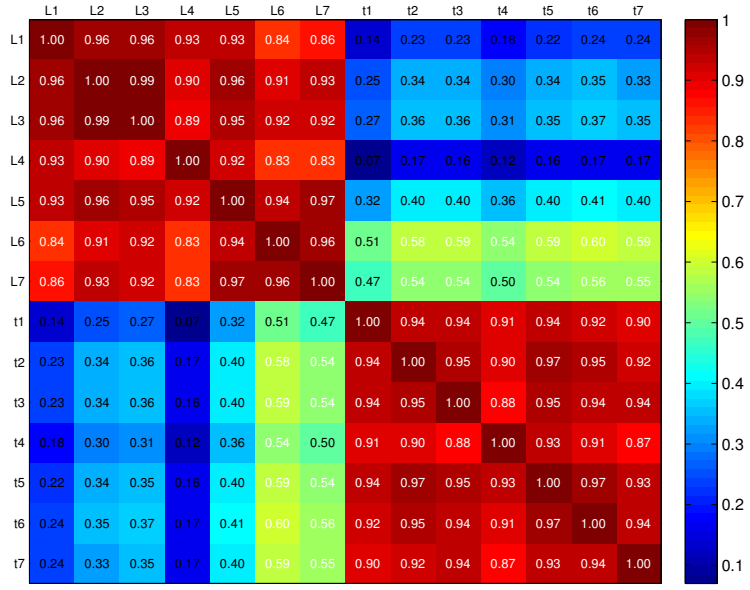

(a) Whole Year

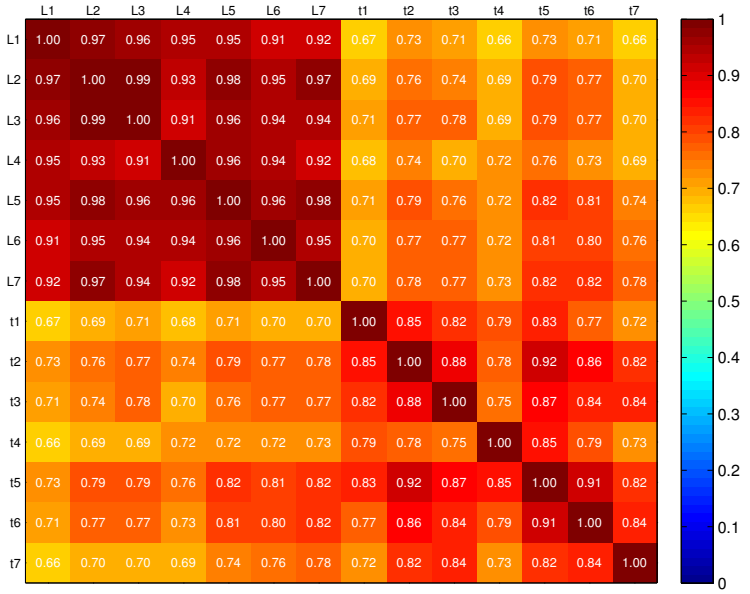

(b) Summer Only

Figure 2.10: Correlations among electricity demand and temperature

time-series models. The methodology of the modeling is based on Jeon et al. (2014) and Mo (2012).

The basic structure of the time-series model is as follows:

$$\text{Temperature}_t = f_T(\text{Deterministic Cycles}_t) + u_t \tag{2.1}$$

$$\log(\text{Wind Speed}_t + 1) = f_W(\text{Deterministic Cycles}_t, \text{Temperature}_t) + v_t \tag{2.2}$$

$$\log(\text{Electricity Demand}_t) = f_L(\text{Deterministic Cycles}_t, \text{Temperature}_t) + w_t \tag{2.3}$$

For $t = 1, 2, \ldots T$, where u_t, v_t and w_t are ARMA(p, q) residuals.

A two-stage estimation method was used for wind speed and electricity demand as a univariate Auto Regressive Moving Average (ARMAX) model with exogenous variables because the deterministic parts of equations showed excessively complicated forms and classic Vector Auto Regression (VAR) models could not come up with feasible solutions. The raw residuals of most models show persistent positive auto-correlations up to 48 hours.

For temperature, the average Pseudo R2 of 99% implies that one-hour ahead forecasts have a 1% error, and the average Adjusted R2 of 78% implies that this forecasting error will increase to 22% for forecasts many hours ahead. In contrast, the equivalent model for Log(Wind Speed+1) has an average Pseudo R2 of 82% and an average Adjusted R2 of only 11% because wind speed does not have strong seasonal and daily patterns and is much harder than the temperature to forecast accurately. The corresponding fit for Log(Load) is good and similar to the temperature with an average Pseudo R2 of 99% and an even higher average Adjusted R2 of 90%. Load and temperature have highly predictable seasonal and daily patterns compared to wind speed.

2.2.4 Simulating Wind and Electricity Demand

Using the models estimated in Section 2.2.3, simulations were performed to create realization profiles of wind and electricity demand for the chosen summer day (Aug-2, 2006). Lagged historical temperature data and corresponding white-noise residuals before the beginning of the simulated day were used to compute the deterministic forecasts of temperature for 30 hours ahead. The simulation treats all initial lagged variables as given, because the initial simulation computed by wind, electricity demand, and temperature all together showed unrealistically high variability in wind and electricity demand. Therefore, this procedure assumes that the system operator has a perfect forecast of temperature, but the forecasting error of wind and electricity demand is high enough to be considered for the day-ahead planning. Using this forecasted temperature data, Monte Carlo analysis was performed for wind and electricity demand to generate 1000 sample realizations of 30-hour wind and demand profiles. (Jeon et al. (2014)).

Figure 2.11 and Figure 2.12 demonstrate 1000 simulated realizations of wind and electricity demand for two locations. Simulated realizations for both wind and electricity demand show that the forecasting error is very small in immediate hours, but it gradually increases, and after approximately 10 hours from the beginning of forecasting, the spread of realization profiles forms a stable level, and the forecasting errors stop increasing.

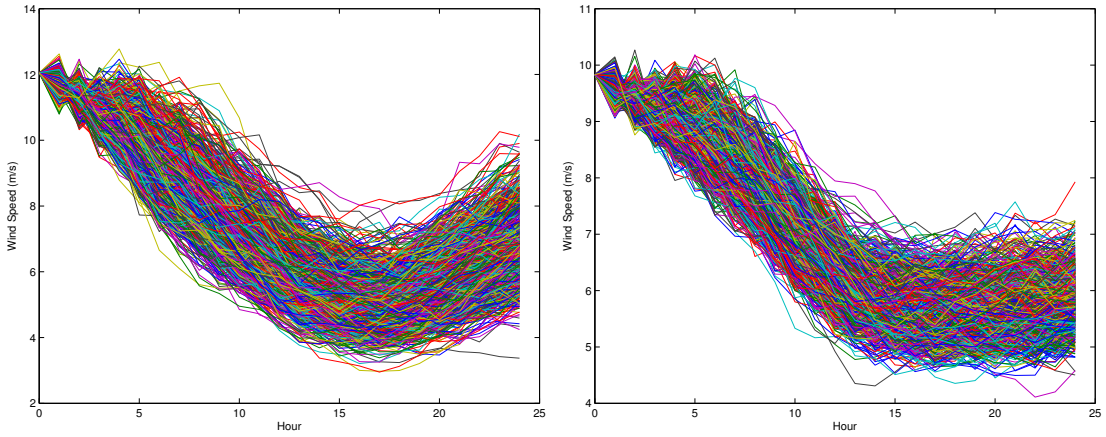

(a) Boston (b) Rochester

Figure 2.11: 1000 simulated realizations of wind speed

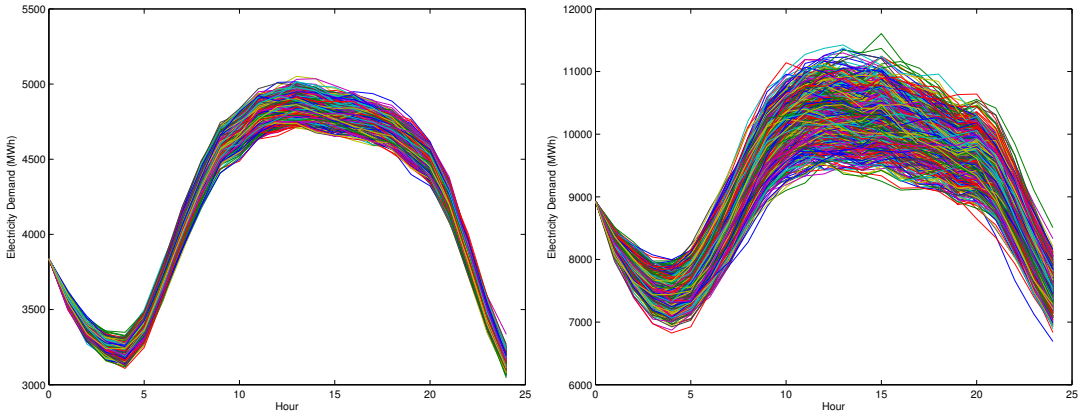

(a) Boston (b) New York City

Figure 2.12: 1000 simulated realizations of electricity demand

2.2.5 Converting Wind Speed to Power

Wind speed is converted to power based on the methodology introduced in the paper, " A Multi-Turbine Power Curve Approach" by Norgaard and Hottlinen (2004). The step-by-step guide of methodology described in this paper is as following:

- Step 1: The wind is characterized in terms of the wind speed distribution, the mean wind speed and the turbulence intensity.

- Step 2: The wind speed time series is adjusted to the relevant hub height and smoothed by a moving block averaging using a time slot representing the propagation time over the area.

- Step 3: The 'smoothed power curve' is found based on a representative standard power curve and the standard deviation of the spatial wind speed distribution, and scaled appropriately to represent the total installed wind power capacity.

- Step 4: The aggregated wind power time series is finally derived by applying the smoothed and scaled power curve to the smoothed and adjusted wind speed time series.

As noted in Step 2, this wind power conversion procedure includes a moving average of the simulated wind speed with both lead and lagged values. This is why the simulation generates forecasts 30 hours ahead. The number of leads and lagged variables are smaller than 5 in most cases, and it is determined by the size of wind farm area as this moving average is applied here to represent the propagation time over the area. The idea of propagation time is based on the logic that the turbines in the large wind farm do not respond to changes in wind speed immediately.

The inputs needed to apply this method are :

1) a wind speed time series representative for the area,

2) a standard wind turbine power curve representative for the wind turbines to be covered, and

3) the dimensions of the area.

Wind turbines used in this study follow the IEC3 standard and have 2MW capacity. Figure 2.13 shows the IEC3 power output of 2MW-capacity wind turbine for different wind speed levels. As shown in this figure, wind speed less than 3 m/s does not generate any power, and it generates at its maximum output level from 12 m/s wind speed. Power output stays at its maximum until 22 m/s of wind speed, and it drops rapidly to zero when it just exceeds 22 m/s. This is because at very high wind speeds, a wind turbine can be damaged, so it protects itself by stopping generation. (Pennock (2012)).

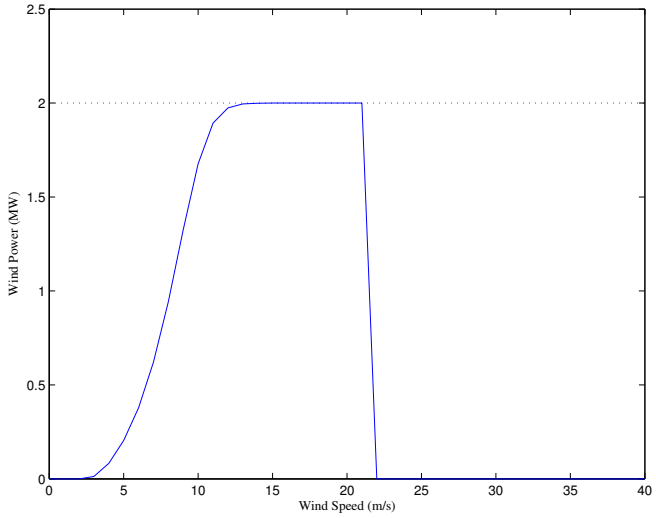

Figure 2.13: IEC3 Power Curve of 2MW-capacity Wind Turbine, Source : Pennock (2012)

The area dimension of each site is based on a description of each site provided by NREL. The area dimensions of all sites included in each group are aggregated and used as area dimensions for the 16 sites representing the whole area in New York and New England.

Figure 2.15 shows the wind power profiles converted from simulated profiles of wind speed in Figure 2.11. Since a moving average method was applied,

wind power profiles show more smooth and persistent shapes.

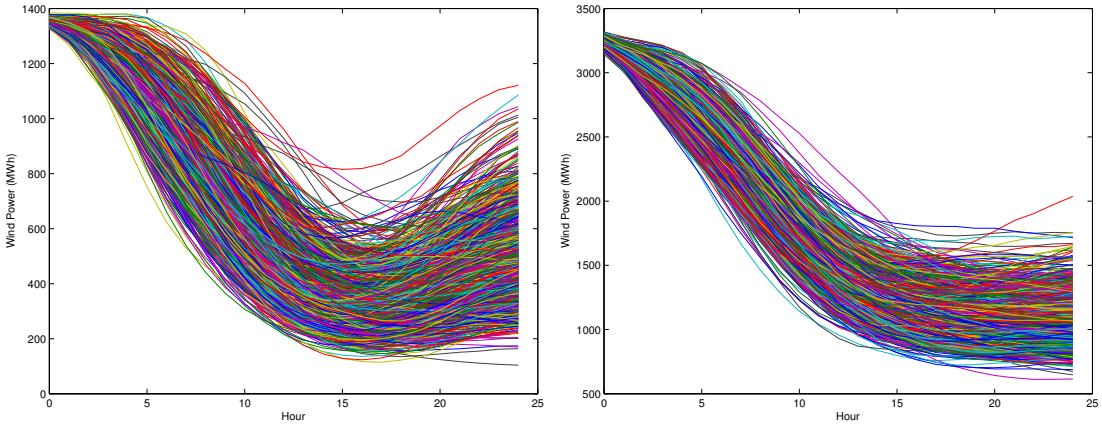

(a) Boston (b) Rochester

Figure 2.14: 1000 realizations of wind power profiles converted from wind speed

2.2.6 Generating Scenarios for Wind and Electricity Demand

The final step is to create five scenarios of 24-hour profiles of wind generation and electricity demand to represent the 1000 simulated samples and to calculate the corresponding transition probabilities from the five scenarios in one hour to the five scenarios in the next hour. These transition probabilities are used as inputs for the Multi-Period SuperOPF used in the empirical analysis. The specific procedure followed for determining the five scenarios for each hour simulated is to cluster values into bins based on the ranked total amount of wind power for all 16 wind sites. Since the 1000 values of total wind generation for each hour are approximately normally distributed, the cut off points are set to correspond roughly to plus and minus two standard deviations and plus and minus one standard deviation. In other words, the highest scenario bin corresponds

to a bin with 2.5% of the sample values and it contains the 25 highest values of total wind generation. In a similar way, the remaining four scenario bins, in ranked order, contained 145 (14.5%), 660 (66%), 145 (14.5%), and 25 (2.5%) sample values, respectively. Therefore, the top two bins represent relatively low probability system states with abundant wind power, and the bottom two bins represent relatively low probability system states with scarce wind power. The large middle bin represents the typical amount of wind power for that hour.

$$Hour1\ to\ Hour2: \begin{bmatrix} 0.6400 & 0.3200 & 0.0400 & 0 & 0 \\ 0.0621 & 0.6621 & 0.2759 & 0 & 0 \\ 0 & 0.0621 & 0.8758 & 0.0621 & 0 \\ 0 & 0 & 0.2759 & 0.6552 & 0.0690 \\ 0 & 0 & 0.0400 & 0.3600 & 0.6000 \end{bmatrix} \tag{2.4}$$

$$Hour2\ to\ Hour3: \begin{bmatrix} 0.5600 & 0.4000 & 0.0400 & 0 & 0 \\ 0.0759 & 0.6483 & 0.2759 & 0 & 0 \\ 0 & 0.0621 & 0.8788 & 0.0591 & 0 \\ 0 & 0 & 0.2690 & 0.6828 & 0.0483 \\ 0 & 0 & 0 & 0.2800 & 0.7200 \end{bmatrix} \tag{2.5}$$

$$Hour23\ to\ Hour24: \begin{bmatrix} 0.8800 & 0.1200 & 0 & 0 & 0 \\ 0.0207 & 0.8345 & 0.1448 & 0 & 0 \\ 0 & 0.0318 & 0.9470 & 0.0212 & 0 \\ 0 & 0 & 0.0966 & 0.8966 & 0.0069 \\ 0 & 0 & 0 & 0.0400 & 0.9600 \end{bmatrix} \tag{2.6}$$

The transition probabilities are shown in Eq (2.4) to Eq (2.6) and determined in the following way. Consider any one of the scenario bins for any chosen hour, $0 < t < 24$. This bin contains sample values that correspond to specific simulated runs, and in the next hour, $t + 1$, those same sample values are distributed

somewhere in the five bins for hour $t + 1$. The proportions of the total number of sample days in the chosen bin for hour t that end up in each bin in hour $t + 1$ determine the transition probabilities. For example, with 25 sample values in the top bin in hour t, the corresponding $t + 1$ values are distributed in the five bins as follows: 20, 5, 0, 0, 0, then the five transition probabilities are 0.8, 0.2, 0, 0, 0, respectively. These probabilities are then weighted by the bin size/1000 = 25/1000. Following the same procedure for the other four bins ensures that the sum of the 25 weighted transition probabilities from the five bins in hour t is equal to one.[1]

As shown in Eq (2.4) to Eq (2.6), the rows in the transition matrix indicate states in the beginning hour and the columns are states in the ending hours: hence, the sum of row elements become 1, meaning that the sum of probabilities that a certain scenario points at the beginning hour transit to all possible scenario points in the ending hour is always 1. The diagonal elements in transition matrixes are dominant. This means that scenarios tend to stay at the state that they are from, thus showing persistence.

$$Hour1\ to\ Hour24 = (Hour1\ to\ Hour2) \times (Hour2\ to\ Hour3) \times ... \times (Hour23\ to\ Hour24)$$

$$= \begin{bmatrix} 0.0394 & 0.1797 & 0.6451 & 0.1188 & 0.0171 \\ 0.0313 & 0.1611 & 0.6567 & 0.1307 & 0.0202 \\ 0.0244 & 0.1441 & 0.6636 & 0.1437 & 0.0242 \\ 0.0205 & 0.1314 & 0.6534 & 0.1628 & 0.0320 \\ 0.0173 & 0.1194 & 0.6375 & 0.1843 & 0.0416 \end{bmatrix} \tag{2.7}$$

[1]These probabilities are actually shrunk even further to allow for low-probability contingencies to occur, and the sum of the transition probabilities into contingency states in hour t and the 25 transition probabilities for intact states from hour t to hour t +1 is equal to one.

Eq (2.7) shows a transition matrix from Hour 1 to Hour 24, indicating the transition from the beginning of the day to the end of the horizon. This transition matrix can be computed by multiplying the series of the transition matrix in a sequential order. This matrix shows the important characteristics of the transition matrix. No matter which scenario one starts from, the probability being in each of the five scenarios 24 hours ahead converges to the probability that these scenario bins are initially defined (2.5%, 14.5%, 66%, 14.5% and 2.5% from scenario 1 through 5). This means that when wind is forecasted, the importance of current information quickly dies down, and finally when wind 24 hours ahead is forecasted, the current information does not matter at all, and the best prediction of the wind state is the mean probabilities for each state.

An important characteristic of the Multi-Period SuperOPF used in this study is that it uses a single set of 5×5×23 transition probabilities to represent the stochastic inputs. This is equivalent to assuming that there are 5 possible intact system states for each hour (i.e., for the intact states, none of the contingencies are realized but the levels of wind generation and electricity demand vary). In general, the weighted transition probabilities derived for total wind generation exhibit substantial persistence from one hour to the next implying that total wind generation that is higher or lower than expected tends to stay that way for a number of periods. However, the levels of wind generation in each scenario must also be specified for individual wind sites, and the same is true for the levels of load for individual load centers. This is accomplished by allocating the sample values into bins for each wind site and load center in exactly the same way as they are allocated into bins for total wind generation, and then computing the average hourly values for each bin for every wind site and load center. Even though this allocation is based on ranked total wind genera-

tion, there is no guarantee for a particular wind site or load center that the 25 highest values, for example, will fall in the top bin. As a result, the ranges of scenario means for locations that are not highly positively correlated with total wind generation will be smaller than they would be if the allocation to bins was based on the ranked values of wind generation and load at each location.

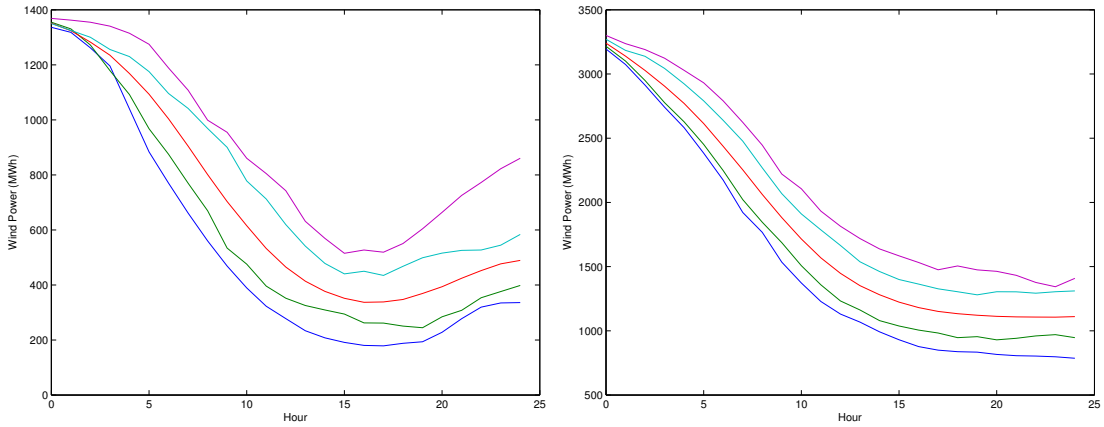

(a) Boston (b) Rochester

Figure 2.15: Five Scenario Profiles from 1000 Simulated Realizations of Wind

For this reason, a new capability has been incorporated into the Multi-Period SuperOPF that can expand the range of the scenario means around the overall mean for the 5 intact scenarios for each hour at every location so that it corresponds to the 95% confidence interval based on the ranked values for that location as shown in Figure 2.15. For example, the highest scenario mean would now correspond to the mean of the 25 highest values at that location, and the lowest scenario mean to the mean of the lowest 25 values. This feature is controlled by two parameters that can take values from 0 to 1. One parameter is for wind generation and the other for load. It should be noted that 1) the overall mean value for the 5 intact scenarios for each hour and each location is always the same regardless of the values of the parameters, and 2) the ranking of the

scenario means for a location that is not highly positively correlated with total wind generation needs not be the same as the ranking of the scenario means for total wind generation.

2.3 Specifications of Deferrable Demands

The deferrable demand has been considered as a demand-side solution for better management of power systems, and the discussions and studies started in the 80's with many papers including Schweppe et al. (1989) and Gellings and Smith (1989). The main idea of deferrable demand is to separate the timing of energy purchases and the time of energy delivery. By doing this, energy consumption in peak hours can be shifted to off-peak hours, and the overall efficiency of the power system increases as the generating capacity required to maintain it can be reduced due to lower peak demand. In addition, more economic generating capacities like nuclear units and hydro units can replace expensive natural gas units. In this study, I analyzed three types of deferrable demands: thermal storage for space conditioning, electric vehicle, and electric water heating. The technical specifications of each deferrable demand and how they are applied to the case study in Chapter 3 are discussed in this section.

2.3.1 Thermal Storage for Space Conditioning

The aggregated storage capacity of thermal storage is set at 17GWh in this study which is approximately a 6.8% penetration level of the total potential cooling electricity demand based on the estimated Temperature-Sensitive De-

Table 2.6: Summary of Thermal Storage Specification

	Thermal Storage
Target Aggregated TS Capacity	17 GWh
Total Aggregated TSD	251 GWh
Penetration Rate	6.8%
TS Capacity of Benchmark Product(Calmac)	30,000 kWh
Ice Building Power (kW)	3,600 kW
Ice Melting Power (kW)	5,000 kW
Ice Building Power Rate (%)	12 %
Ice Melting Power Rate (%)	17 %
Storage Efficiency	86 %

mand(TSD) on the chosen summer day (Aug. 2, 2006). This study assumes that the energy corresponding to 12 hours of average daily Temperature-Sensitive Demand(TSD) can be shifted by thermal storage. The concept of a TSD profile is illustrated in Figure 1.1. This makes the amount of energy replaced by thermal storage bounded at 13.6% of the hourly TSD.

The technical characteristics of thermal storage are based on the products described in the reports by Evapco (EVAPCO (2007)) and Calmac (Hunt et al. (2010)). The hourly ice building power rate is 12% and the hourly ice melting power rate is 16.7% of the total storage capacity. These ice building and melting rates can vary by the number of chillers installed in the thermal storage system. The storage efficiency is 86% which is based on an average energy efficiency ratio(EER) of 8.8 of the thermal storage, compared to an EER of 10.2 for an average conventional AC. In the case study in Chapter 3, thermal storages is distributed in five major demand centers (Millbury, Sandy Pond(Boston), Dunwoodie, New York City, and Buffalo), which are nodes in the 36-bus test network from Figure 2.1. The storage capacity of 17GWh is distributed to each demand center pro-

portional to its electricity demand size.

2.3.2 Electric Vehicle

Table 2.7: Summary of EV Specification

	EV
Target Aggregated EV Capacity	17 GWh
The number of passenger vehicle in NYNE	15,692,624
Total Aggregated EV Capacity in NYNE	169 Gwh
Penetration Rate (%)	10%
Usable battery capacity per vehicle	10.8 kWh
Charger Level (Level1 / Level2)	70/30
Average Charging Power	3.31 kW
Average Charging Power Rate	31%
Average Driving Distance per kWh	4 mile/kWh
Average Commuting Distance (mile)	Rural :36.9, Surburban: 28.8, Urban: 27.2
Storage Efficiency (%)	90%

The specifications of the battery technology for Electric Vehicles (EVs) follow that of a GM Volt 2013. This type of battery is lithium-ion and the usable energy capacity is approximately 65% of the total battery capacity(16.5kWh), which is 10.8kWh. The total number of passenger-size vehicle in NY and NE is 15,692,624 according to State Motor-Vehicle Registrations in 2006, which amounts to an aggregated energy capacity of 17GWh. The EVs are also distributed in the same five major demand centers, proportional to their load size. The average charging efficiency of lithium-ion batteries is 90% (EAC (2008), Keller et al. (2008)). Two types of charging levels are considered using current technology. Level 1 chargers deliver up to 1.44 kW and level 2 chargers deliver up to 7.68 kW (MassDiv (2000)). It is assumed that 70% of level 1 chargers and 30% of level 2 chargers are available in this network, which implies an average of 3.31 kW. The

specified average driving distances for "rural," "suburban," and "center city" are 36.9 miles, 28.8 miles, and 27.2 miles, respectively (Davis et al. (2011)). This analysis specifies 27.2 miles, because EVs are located mostly in major demand centers.

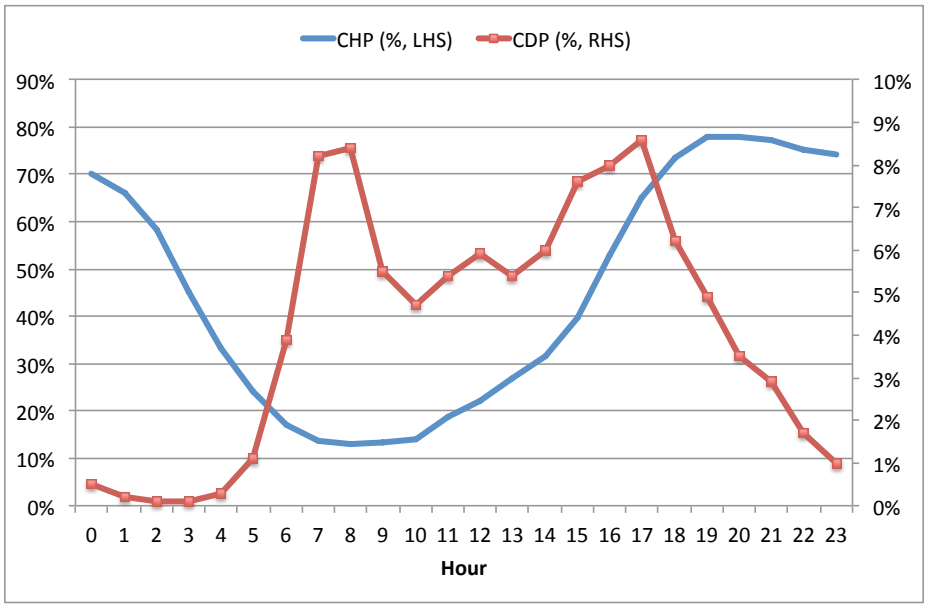

Figure 2.16: Commuter-at-Home Profile(CHP) and Commuter Driving Profile(CDP)

The driving pattern of commuters in this case is based on the 'Commuter Driving Profile' (Parsons and Douglas (2000)); the percentage of commuters at home, determining how many vehicles are connected to the grid and available for charging, is based on the 'Commuter-at-Home Profile' (Valentine et al. (2011)). This case assumes that EVs are connected to smart chargers as soon as the drivers arrive home, and stay connected until they leave for work. This study assumes that there is no charging station at work, so charging only takes place when EVs are at home. Vehicle to Grid(V2G) is not allowed in this case study, and the driving energy efficiency is set at 0.25 kWh/mile.

2.3.3 Electric Water Heating

Table 2.8: Summary of Water Heating Specification

	Electric Water Heating
Target Aggregated Capacity	17 GWh
Heater Tank capacity	80 gallon
Recovery Rate	20 GPH(Gallon Per Hour)
Charging Power	4.5 kW
Storage Efficiency (%)	91%

Electric water heating is commonly used in both residential and commercial buildings, and it works by heating up the water using electric resistance heat at night when electricity prices are low. The hot water is stored in a well-insulated tank and used during the day time when the electricity prices are generaly high. The same 17 GWh of total storage capacity is assumed for water heating in this study. Electricity demand for water heating can be categorized as N-TSD, so similar to thermal storage, the energy corresponding to 12 hours of average daily Non-Temperature Sensitive Demand(N-TSD) can be shifted by electric water heating. The 17GWh of total storage capacity corresponds to 4.4% of the total daily N-TSD on this chosen summer day (Aug. 2,2006). The hourly profile of the energy equivalent (MWh) of the hot water used by customers is assumed to be proportional to the hourly profile for N-TSL at each location. The technical characteristics of the electric water heater are based on a product made by Rheem (www.rheem.com). This product has an 80-gallon tank, a recovery rate of 20 GPH (20 gallons of water can be heated to 90F rising at 4.5kWh in one hour), and a heating efficiency of 91%.

Figure 2.17 illustrates the hourly profiles of energy consumption that can be replaced by three types of deferrable demand at the specified storage capacity

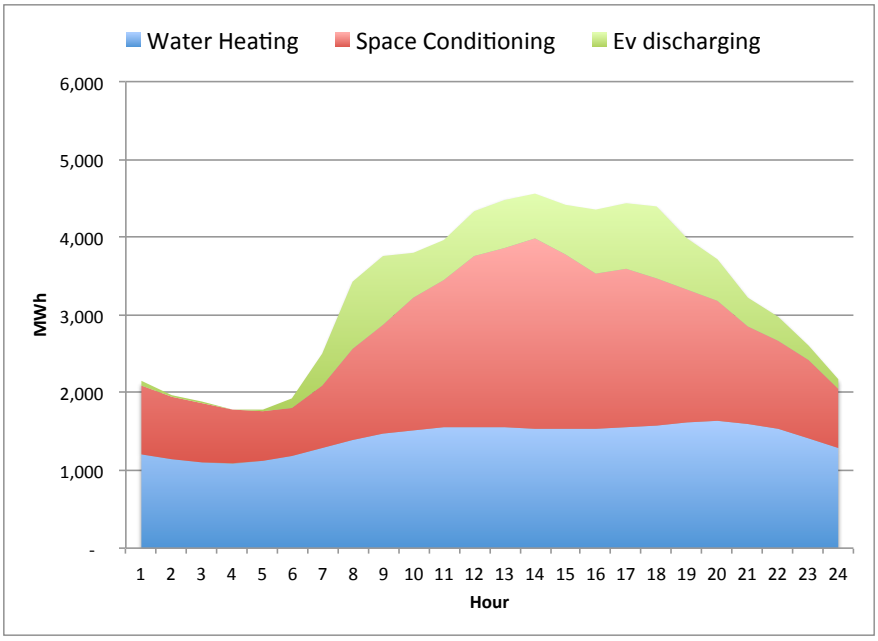

Figure 2.17: Hourly Cumulative Profiles of Energy that can be replaced by three types of deferrable demands

of 17GWh for each deferrable demand. The profile of water heating is proportional to NTSD, and the profile of space conditioning is proportional to TSD as each of them can be classified as N-TSD and TSD, respectively. Hence, the area below the profile of space conditioning is the potential amount of energy that these two types of deferrable demand can move for better system management. The profile of EV discharging shows the amount of energy consumed by EV commuting based on Commuter Driving Profiles shown in Figure 2.16: therefore, this EV discharging is not the resource that a power system can take advantage of, but the fixed energy consumption required to meet the needs of EVs.

2.4 Specification of Utility-Scale Storage

The supply-side utility-scale storage used in this study is Lithium-Ion Energy Storage Systems(ESS) collocated at the wind sites specified in section 2.2. ESS is located in all 16 specified wind farms in New York and New England, and dedicated to support wind generation. The main role of ESS is to help mitigate wind variability and uncertainty by using stored energy in ESS to provide energy in the different wind scenarios and supporting he grid when any contingency event occurs. ESS can also take advantage of price arbitrage by storing abundant wind energy at night when the electricity prices are generally low, and using stored energy at day when prices are high.

In the empirical analysis in Chapter 3, the total capacity of ESS is set at the sum of energy capacity of thermal storage and water heating, which is 34GWh. This ensures a fair comparison between the case with three types of deferrable demand and the case with ESS. The capacity of EV is not added to ESS because EV does not directly help the power system as most of the energy stored is used for commuting. The basic technical specification of ESS follows that of the Lithium-Ion battery described in section 2.3.2. The maximum hourly power available per ESS is set to be 22% of the energy capacity. This is based on the assumption that 85% of level1 and 15% of level2 charging rates are available. Compared to 70/30 (level1/level2) for the EV case, this lower charging rate of 85/15 is assumed because many wind farms are located in rural areas, far from major demand centers and are connected via relatively low capacity transmission lines. The efficiency of lithium-ion batteries used for ESS is 90%.

CHAPTER 3

THE TRUE VALUE OF DEFERRABLE DEMAND AND UTILITY-SCALE STORAGE IN A SMART GRID ENVIRONMENT

3.1 Introduction

Increasing adoption of generation from wind energy in the electric power system is often believed to lead to decreased overall system costs because wind is essentially a free resource, and it is expected to displace fossil-fuel generation. However, this may not be true because characteristics of wind generation which are highly variable and difficult to forecast create additional costs that the system operator needs to consider when planning for the dispatch of conventional generations. These additional costs include the operating costs and capital costs of the reserve generating capacity required to support the uncertainty caused by wind generation. In addition, there is much evidence that there are additional ramping costs mainly related to maintenance costs for physical stress on conventional generators caused by wind generation due to frequent and rapid changes of dispatch level to adopt more wind energy. This evidence comes especially from counties with a high penetration of wind generation such as Ireland and Denmark.

There is also a movement in the US to recognize the impact of high uncertainty and variability of wind generation on the power system. The California ISO recently mentioned the need of ”Flexible Capacity” to address the added variability and uncertainty of variable energy sources and started working to develop flexible capacity requirement and procedures for assigning these requirements to individual participants in the electricity market. (CAISO (2014))

The additional challenges associated with wind generation include the congestion on the transmission network caused by transferring high volume of wind generation from wind farms to major cities where electricity demand is concentrated. This high congestion prevents wind generators from getting paid at high nodal prices formed in major cities because nodal prices at wind farms are normally set at much lower prices. Because abundant wind generation is concentrated in this node and the electricity demand in this rural areas, nodal prices remain relatively low. In particular at night when wind is strong, nodal prices can go below zero resulting in wind generators getting paid at negative prices. To solve this problem and run the wind farms more effectively, a large investment is needed for transmission capacity to connect wind farms and major cities, but the cost of upgrading the transmission capacity is significantly high, and it is not an easy decisions that local ISOs can make.

An Energy Storage System(ESS) can help solve many of the rising challenges caused by highly variable wind generation. Many projects have been carried out including one by AES in Laurel, West Virginia where they installed energy storage at wind farms and supported wind generation. The capacity of wind farm in Laurel is 98MW and the capacity of installed storage is 32MW, making it one of the largest projects of its kind.(Kumagai (2012)) This supply-side energy storage dedicated to wind generation is used for better operation of wind generators by mitigating the variability and uncertainty of wind generation and providing energy services like moving wind energy stored at 3 am to 3 pm when the electricity demand is peak and generating capacity is needed the most. However, this supply-side storage dedicated to wind generation which is mostly a type of Lithium Ion or Compressed Air Energy Storage (CAES) is very expensive, and it is difficult to justify the initial investment cost.

Whereas, as briefly mentioned in Chapter 1, the demand-side solution including "deferrable demand" can be an effective alternative to the supply-side solution. Space conditioning using thermal storage or water heating using electric water heater with insulated tanks can be considered as deferrable electricity demand. The main characteristics of this deferrable demand is that it can separate the timing of the energy purchase and the time of energy delivered. The electricity consumption for space conditioning and water heating, on average, is approximately 26.1% and 9.1% of the total electricity demand in the US, respectively. (EIA (2001)) The significant portion of electricity demand has a potential to be deferred by thermal storage and electric water heaters, and it can provide the ramping service required by the high variability of wind generation as well as peak load reduction by shifting peak demand to off-peak hours. The cost of deferrable demand is much lower than the supply-side storage dedicated to wind farms because the cost of storage is divided into two processes: providing its own utility and serving the grid.

There is an additional benefit from implementing deferrable demand in the power network with high penetration of wind generation. Deferrable demand can be an effective alternative to the large transmission capacity upgrade needed by wind generation. Most network congestion occurs during peak hours when large wind generation needs to be transferred from wind farms to major cities. However, if deferrable demand is implemented in the major cities where the potential resource of deferrable demand is high, deferrable demand like thermal storage or electric water heaters store wind energy during the night, when wind generation is generally more abundant and network congestion is low. This stored energy in the deferrable demand owned by customers living in major cities can serve the need when those services are needed at peak load

hours. Hence, deferrable demand increases the efficiency of wind generation and the transmission network at the same time and help avoid another large investment in generating capacity and transmission capacity. The economic benefit of deferrable demand as an alternative to a transmission capacity upgrade is analyzed in Lamadrid et al. (2014), the paper that I co-authored.

The primary objective of this chapter is to estimate the benefit of different types of storage capacity in the power system with a high penetration of wind capacity. The benefit of storage is evaluated from three main perspectives, by installing storage capacities, 1) how much more wind generation is dispatched to the network, 2) how much reserve costs are reduced, and 3) how much capital cost of installing conventional generating capacity is saved. Supply-side storage and demand-side storage are used and analyzed in different cases. Utility-scale Lithium-Ion batteries collocated at wind farms is used for supply-side storage. For demand-side storage, three different types of deferrable demand are used: electric water heaters, thermal storage for space conditions, and electric vehicle (EV). Those types of deferrable demand capacities are located in major cities and help integrate more wind generation to the network and reduce the system cost.

This study also evaluates electricity payments for customers with different types of deferrable demand capabilities by estimating each customer's contributions to lower the energy, reserve and capacity costs. Finally, this study presents how much benefit the different types of customers can receive from different deferrable demand capability and how these different payments will provide the appropriate economic incentive for customers.

The case study applied in this study uses a new Security-Constrained Opti-

mal Power Flow (SCOPF) developed at Cornell University, named Multi-Period SuperOPF and a reduced form of the power system network in the Northeast Power Coordinating Council (NPCC) from Allen et al. (2008). There are three key features that Multi-Period SuperOPF considers when optimizing the power system. The first feature is that the stochastic characteristics of potential wind generation and electricity demand at each sites is specified, and probability-assigned contingency events are also defined to analyze the power system in some pre-specified system failure situations. The second feature is that the hourly dispatch pattern of energy and reserve for all conventional generation units are determined simultaneously and endogenously given the restrictions of the required operating reliability standard and stochastic inputs. The final feature is that the ramping cost that represents wear-and-tear costs on conventional generating units mostly caused by variable wind generation is implemented in the objective function and affects the decisions on the optimal dispatch solution. The idea of wear-and-tear cost is based on the physical stress imposed on conventional generating units by rapid changes in the dispatch point, so this stress becomes far more significant when conventional generators need to adopt highly variable wind generation.

3.2 Formulation of Multi-Period SuperOPF

A Security Constrained Optimal Power Flow(SCOPF) developed at Cornell University is used for the analysis. This power system simulation platform named Multi-Period SuperOPF is developed based on the architecture of MATPOWER (Zimmerman et al. (2011)). The theoretical backgrounds for security-constrained optimal power flow and location-based scheduling and pricing for

energy and reserves are based on the papers by Chen et al. (2005b) and Thomas et al. (2008). The Multi-Period SuperOPF is the second-generation SuperOPF developed at Cornell University, and the framework of the first generation SuperOPF can be found in Lamadrid et al. (2008). Most of information regarding Multi-Period SuperOPF presented in this section is based on the "Multi-Period SuperOPF (SuperOPF 2.0) User's Manual" written by Ray Zimmerman and Carlos Murillo-Sanchez in 2013.

The objective function of Multi-Period SuperOPF is to minimize the expected sum of the total system cost for a set of stochastic scenarios of potential wind generation and load, and a set of defined contingency scenarios for a 24-hour horizon. Various types of storage capacities including utility-scale storage and deferrable demand can be implemented in this framework. Eq 3.1 shows the simplified formulation of the objective function and Table 3.1 shows the definition of notations.

$$
\begin{aligned}
\min_{G_{itsk},R_{itsk},\mathrm{LNS}_{jtsk}} \sum_{t\in\mathscr{T}}\sum_{s\in\mathscr{S}^t}\sum_{k\in\mathscr{K}}\pi_{tsk}\Bigg\{\sum_{i\in\mathscr{I}}\Big[C_{G_i}(G_{itsk})+ \\
\mathrm{Inc}^{+}_{its}(G_{itsk}-G_{itc})^{+}+\mathrm{Dec}^{-}_{its}(G_{itc}-G_{itsk})^{+}\Big]+ \\
\sum_{j\in\mathscr{J}}\mathrm{VOLL}_j\mathrm{LNS}(G_{tsk},R_{tsk})_{jtsk}\Bigg\}^{[1]}+ \\
\sum_{t\in\mathscr{T}}\rho_t\sum_{i\in\mathscr{I}}[C^{+}_{R_{it}}(R^{+}_{it})+C^{-}_{R_{it}}(R^{-}_{it})+C^{+}_{L_{it}}(L^{+}_{it}) \\
+C^{-}_{L_{it}}(L^{-}_{it})]^{[2]}+\sum_{t\in\mathscr{T}}\rho_t\sum_{s_2\in\mathscr{S}^t}\sum_{s_1\in\mathscr{S}^{t-1}}\sum_{i\in\mathscr{I}^{ts_20}} \\
[\mathrm{Rp}^{+}_{it}(G_{its_2}-G_{its_1})^{+}+\mathrm{Rp}^{-}_{it}(G_{its_2}-G_{its_1})^{+} \\
+f_s(p_{\mathrm{sc}},p_{\mathrm{sd}})]^{[3]}
\end{aligned}
\tag{3.1}
$$

The objective function can be separated and explained largely by three parts.

Part [1] computes the expected sum of the generation cost at its dispatch point, and Value of Lost Load (VOLL) can be defined for Load Not Served(LNS), so that optimization allows load shedding if it is economically efficient. Part [2] calculates the costs related to the reserve capacity needed for contingency scenarios or load following changes to cover wind variability. Part [3] computes the wear-and-tear ramping cost that represents the cost related to physical stress on conventional generating units caused by rapid and frequent changes in the dispatch level, mainly for mitigating wind variability.

Table 3.1: Definition of Variables, simplified Formulation

$\mathscr{T}$	Set of time periods considered, n_t elements indexed by t.
$\mathscr{S}^t$	Set of scenarios in the system in period t, n_s elements indexed by s.
$\mathscr{K}$	Set of contingencies in the system, n_c elements indexed by k.
$\mathscr{I}$	Set of generators in the system, n_g elements indexed by i.
$\mathscr{J}$	Set of loads in the system, n_l elements indexed by j.
π_{tsk}	Probability of contingency k occurring, in scenario s, period t.
ρ_t	Probability of reaching period t.
G_{itsk}	Quantity of apparent power generated (MVA).
G_{itc}	Optimal contracted apparent power generated (MVA).
$C_G(\cdot)$	Cost of generating $(\cdot)$ MVA of apparent power.
$\text{Inc}^+_{its}(\cdot)^+$	Cost of increasing generation from contracted amount.
$\text{Dec}^-_{it}(\cdot)^+$	Cost of decreasing generation from contracted amount.
VOLL_j	Value of Lost Load, ($).
$\text{LNS}(\cdot)_{jtsk}$	Load Not Served (MWh).
$R^+_{it} < \text{Ramp}_i$	$(max(G_{itsk}) - G_{itc})^+$, up reserves quantity (MW) in period t.
$C^+_R(\cdot)$	Cost of providing $(\cdot)$ MW of upward reserves.
$R^-_{it} < \text{Ramp}_i$	$(G_{itc} - min(G_{itsk}))^+$, down reserves quantity (MW).
$C^-_R(\cdot)$	Cost of providing $(\cdot)$ MW of downward reserves.
$L^+_{it} < \text{Ramp}_i$	$(max(G_{i,t+1,s}) - min(G_{its}))^+$, load follow up (MW) t to $t+1$.
$C^+_L(\cdot)$	Cost of providing $(\cdot)$ MW of load follow up.
$L^-_{it} < \text{Ramp}_i$	$(max(G_{its}) - min(G_{i,t+1,s}))^+$, load follow down (MW).
$C^-_L(\cdot)$	Cost of providing $(\cdot)$ MW of load follow down.
$\text{Rp}^+_{it}(\cdot)^+$	Cost of increasing generation from previous time period.
$\text{Rp}^-_{it}(\cdot)^+$	Cost of decreasing generation from previous time period.
$f_s(p_{\text{sc}}, p_{\text{sd}})$	Value of the leftover stored energy in terminal states.

This Multi-Period SuperOPF determines the optimal dispatch decision for both energy and reserves indigenously subject to demand constraints, system constraints such as generating capacities and ramping capabilities and network constraints such as transmission line capacity. The basic scheme of optimization is day-ahead market optimization and the system operator runs optimization with best available information at that point.

3.3 Specification of Network and Power System Inputs

Data for power system specifications and network specifications used in this study are calibrated using mostly publically available sources. This public information is modified and simplified to consider the computational limitations and fit the empirical analysis performed in this study. Descriptions of the test network, wind data, electricity demand data, and storage information used in this study are thoroughly presented in Chapter 2. In this section, input descriptions that are already discussed in Chapter 2 are left with reference points to avoid redundancy.

3.3.1 The NPCC Test Network

Figure 2.1 shown in Section 2.2 is the network map used in the case study, and it is a reduced form of the Northeast Power Coordinating Council (NPCC) network provided by Allen et al. (2008). This network is modified and simplified to include information about transmission capacities and generating units at each bus from the PowerWorld Corporation.

Table 3.2 summarizes the capacity of generating units by each fuel type and each region classified by the Regional Transmission Organization (RTO). The total capacity of conventional generating units is approximately 144GW, and the total system electricity demand at the peak is approximately 138 GWh. The distribution of generating the unit fuel type is different by region due to each RTO's policy. Fuel costs for each generator take a quadratic or piecewise linear function form, and they vary by region and bus. Natural gas costs are generally high in New York and coal costs are high in New England.

Table 3.2: Summary of Generation Capacity and Load

	Capacity per Fuel Type (MW)					Total Cap.	Load
Location (RTO)	coal	ng	oil	hydro	nuclear		
isone	1,840	9,219	4,327	1,878	5,698	22,962	23,847
marit.	2,424	1,072	22	641	641	4,800	3,546
nyiso	4,557	18,185	5,265	7,345	4,714	40,066	38,274
ont.	5,287	3,594	0	779	12,249	21,910	21,158
pjm	14,453	14,611	8,915	2,604	12,500	53,083	51,588
quebec	0	0	0	800	0	800	0
Total	28,562	46,681	18,530	14,048	35,802	143,707	138,412
LF R.C.[b]	30	10	10	60	60		

[a] Values shown are taken as peak values.

[b] Load-Following Reserve Costs ($t/MW).

The load following reserve costs are assigned by fuel type and they use linear cost functions for the dispatch level change for consecutive hours for each generating unit. High costs are assigned for generators providing base load such as hydro and nuclear generator. Generating units providing electricity for peak hours like natural gas and oil units have low load-following reserve costs as their ramping capability is much better than nuclear or hydro units and it takes relatively low costs to ramp up or down in a short time period.

Seven regions for different electricity demand patterns are defined in New York and New England as described in section 2.2.1. Each region has its own profile represented by probability-assigned multiple scenarios. The power system optimization is required to meet this specified electricity demand. However, Value of Lost Load (VOLL) is defined as having very high costs ($5,000/MWh for rural areas and $10,000/MWh for urban areas), so shedding load is allowed if it is economically feasible.

3.3.2 Specifications for Stochastic Wind Generation, Stochastic Electricity Demand, Deferrable Demand, and Utility-Scale Storage

The wind data used in this study is from the Eastern Wind and Transmission Study (EWITS) by the National Renewable Energy Laboratory (NREL), and it is simulated data measured at every 10 minutes and 80m height from 2004 to 2006. Electricity demand data are historical data from NYISO and ISO-NE. The specifications of how wind sites and electricity demand regions are discussed, and 16 wind sites and 7 demand regions are defined in section 2.2.1. For these wind sites and demand regions, different time-series econometrics models are estimated using univariate Auto Regressive Moving Average (ARMAX) models (section 2.2.3), and then 1000 samples of wind and electricity realizations for each site are simulated (section 2.2.4). Then simulated wind realizations are converted to wind power using the "Multi-Turbine Power Curve Approach" by Norgaard and Hottlinen (2004) described in section 2.2.5. Finally, five scenarios for wind power and electricity demand profiles that include characteristics of

all 1000 sample realizations are generated using the bin method, and the corresponding transition probability matrix that defines the probability of moving between scenarios from hour to hour is described in section 2.2.6

Specifications of three types of deferrable demands, thermal storage for space conditioning, electric vehicle and electric water heater are described in section 2.3.1, 2.3.2, and 2.3.3, respectively. These types of deferrable demands are distributed in five major cities, which are Millbury, Sandy Pond(Boston), Dunwoodie, New York City, and Buffalo. Specifications of utility-scale storage collocated at wind farms are discussed in section 2.4.

3.4 Results of Empirical Study

This section summarizes the system costs and payments for different types of customers for meeting specified stochastic demand profiles for a 24-hour period for seven different cases on a hot summer day using the network illustrated in Figure 2.1. In earlier studies, the impact of renewable generation on system costs was mainly analyzed based on the financial benefit that customers can make in wholesale markets by reducing the electricity price because operating costs of renewable generation are basically zero. However, these cost savings in the wholesale market are only part of the benefits, with more and possibly bigger cost savings coming from the capacity market. A decrease in the peak capacity needed to maintain reliability by dispatching renewable generation considerably lowers the total capacity cost needed to pay for generators. Ignoring these capacity cost savings would result in significantly underestimating the effect of renewable generation on the system costs. Hence, to evaluate the correct cost

savings that the system faces, analysis in this paper considers 1) the true operating cost that conventional generators face and also is largely affected by the amount of wind generation dispatched and 2) the maximum conventional generation capacity needed to meet the electricity demand at peak hours and maintain system reliability. Regarding the effect of 1), the relationship between the operating cost of conventional generation and the amount of wind generation dispatched is not simple. The fuel cost of conventional generation can decrease if more wind generation replaces fossil fuel generation, but the higher wind generation can incur higher reserve costs for conventional generators because high variability in wind generation needs to be managed.

3.4.1 The Structure of the Case Study

The main focus of this empirical study is to analyze the interaction between highly variable wind generation and different types of storage, and their impacts on system costs. This case study analyzes the system results of the following seven cases:

1. Case 1: No Wind, base case
2. Case 2: 16 GW of Wind Capacity at 16 locations as specified in section 2.2.1
3. Case 3a: Case 2 + 17 GWh of Water Heating, 17 GWh of Thermal Storage, and 17GWh of EV at 5 demand centers
4. Case 3b: Case 2 + 17 GWh of Water Heating and 17 GWh of Thermal Storage at 5 demand centers
5. Case 3c: Case 2 + 17 GWh of Water Heating and 17 GWh of EV at 5 demand centers

6. Case 3d: Case 2 + 17 GWh of Thermal Storage, and 17 GWh of EV at 5 demand centers
7. Case 4: Case 2 + 34 GWh of ESS collocated at 16 wind sites

Case 1 analyzes the base case of the NPCC test network. This case only has conventional generators and faces stochastic electricity demand. Case 2 adds 16GW of wind capacity to Case 1 and is distributed among 16 locations specified in section 2.2.1. In Case 3, three types of deferrable demands, electric water heater with an insulated tank, thermal storage for space conditioning and electric vehicle, are added to Case 2 in five major cities described in section 2.3. Case 3a installed 17 GWh of each of the three types of deferrable demands, and Case 3b has 17GWh of water heaters and thermal storage. Case 3c has water heaters and EV, and case 3d has thermal storage and EV. In Case 4, 34GWh of utility-scale storage is added to Case 2, which are collocated at 16 wind farms.

The comparison between Case 1 and Case 2 is expected to illustrate the effect of adding large wind capacity to the grid. These cases show how wind generation displaces fossil fuel generation and how much the system cost is increases due to its variability to maintain system reliability. The comparisons between Case 2 and Case 3a-Case 3d, and between Case 2 and Case 4 show the effects of different types of storages on the power system with high penetration of wind generation. They show how different types of storages mitigate wind variability and increase overall conventional generation efficiency by shifting expensive peak demand to off-peak hours.

3.4.2 Impacts of Different Types of Storages on System Costs

Table 3.3 highlights the important daily system results for seven cases. The results are displayed as differences between relevant cases to make the comparison clearer and more intuitive. The 'Expected Outcome' section of Table 3.3 summarizes the amount of wind generation, conventional generation, and reserve capacities required to meet the reliability standard. The 'Composition of Wholesale Costs' section of this table shows the composition of system operating costs derived from the objective function of Multi-Period SuperOPF. Level values are presented for the base case, Case 1, and the difference between Case 2 and Case 1 is presented to analyze the effects of adding wind capacity to the network. Then the differences between Case 3 to 4 and Case 2 are illustrated to analyze the effects of adding different types of storage to the network with wind capacity. Since the model defines five scenarios for wind and electricity demand and ten contingency events, optimum solutions for dispatch patterns are determined for all 15 states for each hour of the day. The expected outcomes noted in Table 3.3 are expected values over these 15 states of outcomes with corresponding state probabilities.

The amount of wind generation dispatched in Case 2 is about 12% of the amount of conventional generation in Case 1 and this basically displaces conventional generation in Case 2. The ramping reserves required by the system increases about 50% due to high wind variability. When storages are added to the grid with high penetration of wind generation, the most noticeable change is significant reduction in the amount of reserves needed even though the amount of wind generation dispatched increases more than 5,000 MWh. This means that wind variability is largely controlled and mitigated by storages and stor-

Table 3.3: Daily Summary of System Results

	c1	(c2 - c1)	(c3a - c2)	(c3b - c2)	(c3c - c2)	(c3d - c2)	(c4 - c2)
Expected Outcome (MWh/day)							
E[Wind Generation]	-	144,258	5,651	5,068	5,263	4,354	5,659
E[Conventional Generation]	1,193,334	-144,256	8,454	-2,444	7,490	8,488	-2,883
Additional Load from EV	-	-	10,682	-	10,682	10,682	-
LF Ramp-Up Reserve [a]	23,150	14,161	-18,979	-17,437	-14,921	-14,809	-19,541
LF Ramp-Down Reserve [a]	27,222	7,851	-18,052	-17,010	-13,639	-13,591	-15,817
Contingency Reserve	24,530	1,303	-24,159	-24,166	-20,659	-22,948	-22,996
E[Load Shed]	11	-3	-7	-7	-3	-5	-8
Composition of Wholesale Costs ($1000/day)							
E[Generation Cost]	55,682	-12,891	-276	-1,123	-89	104	-1,433
E[Ramp Wear Cost]	62	33	-60	-51	-48	-40	-56
LF Ramp-Up Reserve Cost	222	184	-230	-210	-186	-176	-237
LF Ramp-Down Reserve Cost	260	89	-186	-176	-143	-136	-164
Contingency Reserve Cost	120	6	-118	-118	-101	-112	-112
Other Costs	0 0	68	75	47	84	33	
E[Total Operating Cost]	56,346	-12,579	-802	-1,602	-520	-276	-1,968
E[Net Revenue for CG][b]	79,912	-26,193	3,430	1,131	2,723	457	3,470
E[Net Revenue for WG][b]	-	9,974	2,098	1,335	1,491	829	2,379
E[Net Revenue for ISO]	9,789	-117	-484	-291	-85	60	-686
E[Total Wholesale Cost]	146,047	-28,915	4,242	573	3,609	1,071	3,195
E[Load Not Served] * VOLL[c]	56	-14	-36	-35	-16	-27	-40
E[Total Cost for Customers]	146,103	-28,929	4,206	538	3,593	1,043	3,155

[a] Load-Following Ramp Reserve.

[b] Conventional Generation, Wind Generation.

[c] Value of Lost Load.

ages make wind generation more efficient by minimizing the amount of wind spilled.

Due to the additional load purchased by EV owners, it is difficult to compare between Case 3 with EV and Case 4. However, the comparison between Case 3b and Case 4 provides direct comparison between cases with deferrable demand devices and ESS as the total capacity of deferrable demand in Case 3b

is the same as ESS capacity in Case 4, and both cases face the same electricity demand profiles. This shows that ESS collocated at wind farms is more effective in reducing the ramping reserve needed and accepting more wind generation to the grid. This was expected because ESS in Case 4 is dedicated storage to maximize the utility of wind generation, whereas the utility of deferrable demands in Cases 3 is shared between its own role such as water heating or space conditioning and serving the grid. Comparing Case 3a and Case 3b to assess the effect of EVs on the power system, EVs help take in more wind generation by charging batteries using spilled wind energy, but its capability to mitigate wind variability is not as good as water heaters and thermal storage since the amount of reserve needed is larger. In terms of reduction in operating cost, ESS in Case 4 is the biggest winner. It reduces the total operating costs by almost $2 million/day compared to Case 2. In contrast, the deferrable demand devices in Case 3b which has the equivalent amount of capacity to Case 4, 34GWh, reduces the costs by $1.6 million/day.

Figure 3.1 illustrates the hourly expected generation by different fuel types for four cases. The amount of expected generation for each hour is represented by color: red for nuclear, blue for hydro, yellow for coal, sky blue for natural gas, gray for oil, and green for wind generation. As shown in Case 1, nuclear, hydro and coal generators which are low-cost generation resources are providing base generation as their profiles and hardly move from hour to hour. Natural gas and oil generators provide most of the ramping services by moving up and down to meet time-varying electricity demand. In Case 2, wind generation mostly displaces expensive natural gas and oil generation as expected. Wind is generally more abundant at night, so the green area is thicker in the early hours than peak hours. To take advantage of large wind generation during the early

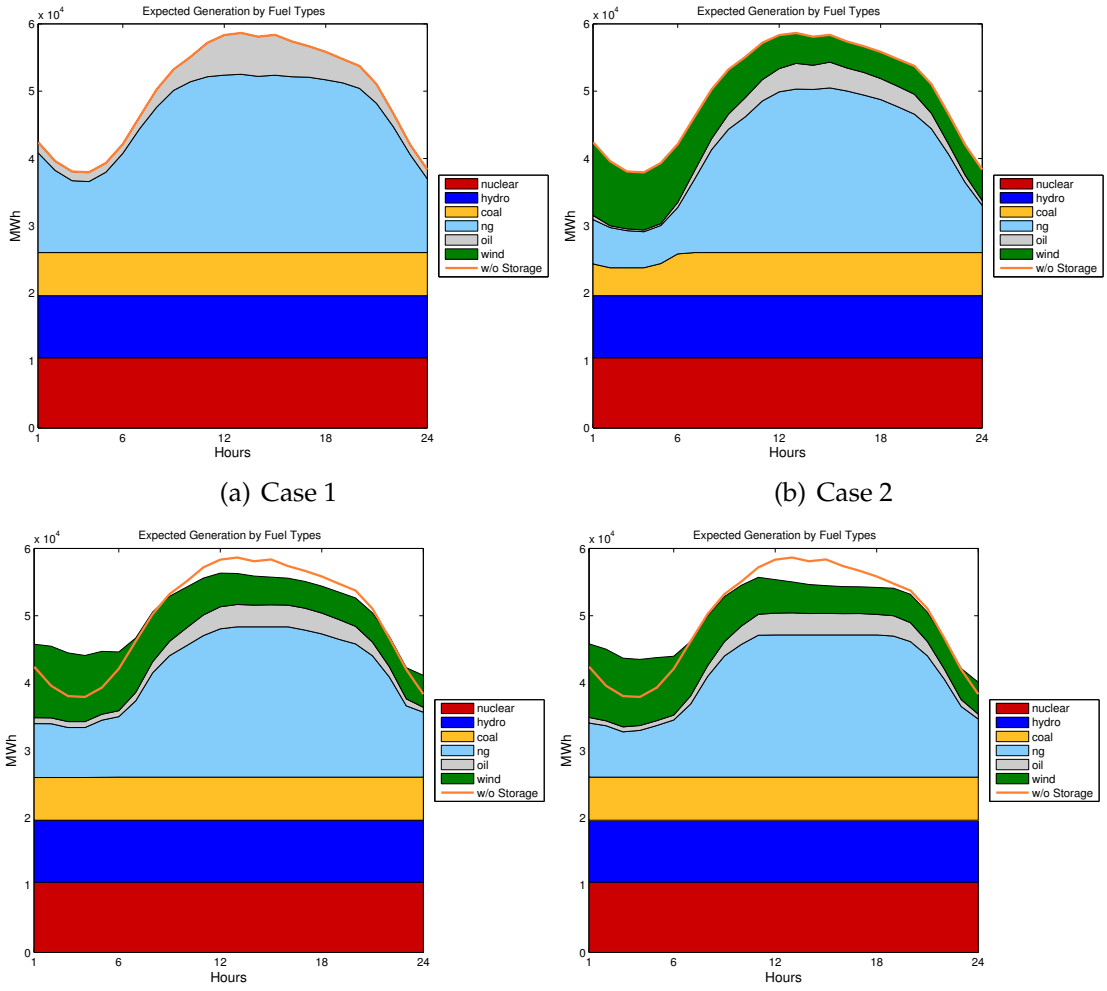

(a) Case 1

(b) Case 2

(c) Case 3a

(d) Case 4

Figure 3.1: Expected Generation Profiles by Different Fuel Types

hours, the system is ramping down coal generators and taking as much wind as it can take.

The orange line in Case 3a and Case 4 shows the pattern of total conventional generation when there are no storages, so the difference between the orange line and the top of colored area is the action by storage capacities. If the orange line falls below the colored area like in the early hours in Cases 3 and 4, storages are purchasing electricity by charging batteries, and if the orange line

is above the colored area like in peak demand hours in Cases 3 and 4, storages are using or selling electricity back to the grid by discharging. In both Cases 3a and 4, wind generation is more dispatched than in Case 2, especially during early hours. Storages take advantage of the abundant wind energy during the early morning hours by charging very low nodal prices. This charged energy is mostly used during peak hours around 1pm when the nodal prices are generally highest. This Figure 3.1 illustrates well that storages contribute to the system by 1) dispatching more wind and displacing more convention generation, 2) providing cheap stored energy at expensive peak hours, 3) decreasing the reserve capacity needed by mitigating wind variability and 4) reducing the peak generating capacity required to maintain system adequacy.

Figure 3.2 shows the hourly range of conventional generation in the different states of the system (the horizontal bars are the expected levels) for Case 2, Case 3a and Case 4, respectively. These vertical lines are the ranges of conventional generation dispatch that the system is required to cover to meet reliability. Therefore, the longer vertical line means more operating reserves are needed. The ranges of conventional generation in Case 2 are relatively large because conventional generators provide all of the ramping needs to accommodate wind variability and contingencies. In contrast, the ranges of conventional generation in Cases 3a and 4 are significantly reduced because both deferrable demands and ESS are very effective in mitigating the wind variability and help reduce the operating reserve needed. For instance, the difference in the ranges between Case 2 and Case 3a at peak hours is approximately 3,000MW, which corresponds to around 5% of the maximum conventional generation needed at the peak load. Consequently, much less reserve capacity is needed to maintain system reliability when storage is available. The overall conclusion is that when

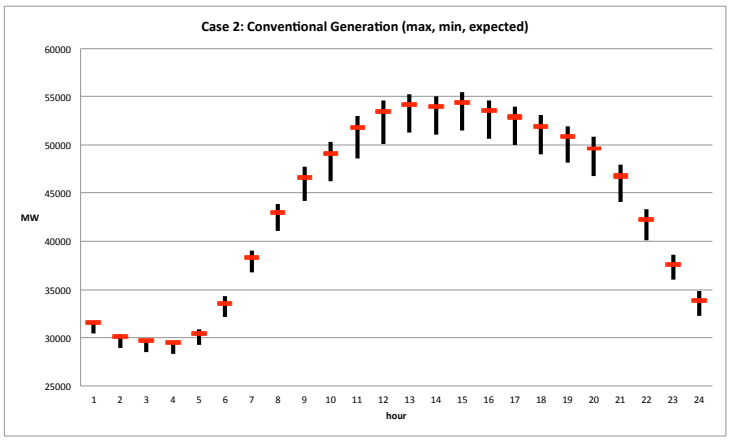

(a) case 2

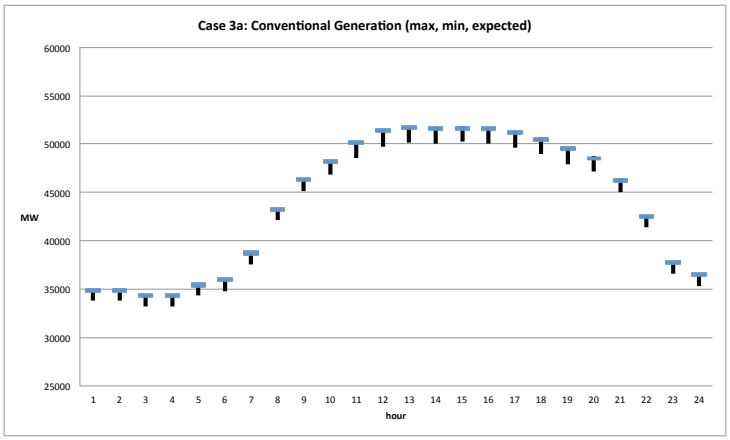

(b) case 3a

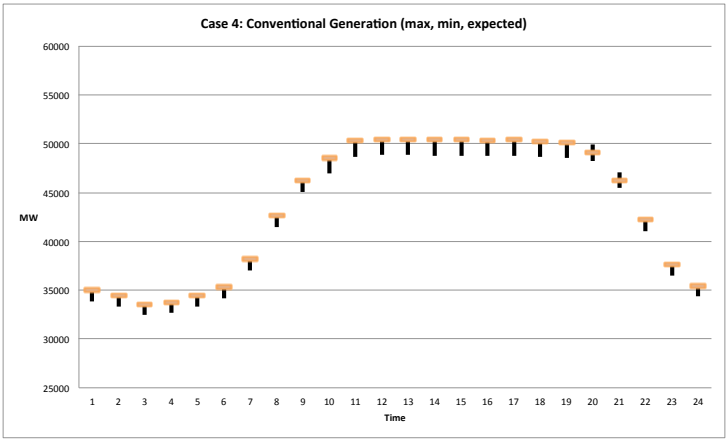

(c) case 4

Figure 3.2: Range of Conventional Generation at max, min and expected

a substantial amount of wind capacity is introduced, the ramping costs of mitigating wind variability are significant and storage is very effective to reduce these costs.

Table 3.4 summarizes peak load hour outcomes of conventional generation and storages. The reduction in conventional generation at the peak hour in Case 3 and Case 4 is because deferrable demand and ESS are actively replacing conventional generation at the peak hour. Thermal storage helps reduce more peak demand than electric water heaters. EVs do not contribute to lower peak demand at all since V2G capability is not allowed for EVs in this case study, so it can not reduce peak system load by selling energy in the battery back to the grid. The 'Capital Cost' part illustrates the total capital cost that each case needs to bear by considering the capital cost of conventional generation based on peak load and the capital cost of storage computed based on the installation cost, maintenance cost, and life cycles of each storage type. Among the three cases in Case 3, only Case 3b shows positive net savings in the total capital costs which means that the capital cost savings in conventional generating capacity at the peak hour is larger than the capital costs of water heaters and thermal storage. In the other cases in Case 3, the net savings in the total capital cost are all negative due to high capital cost of Lithium-Ion batteries used in EVs. However, this high capital cost of EV is compensated by the gasoline cost savings shown in Figure 3.3. The net savings of the total capital cost of ESS in Case 4 are also a loss due to the high capital costs of ESS.

Figure 3.3 illustrates the net savings for the total system costs by considering the savings in the operating costs (generation cost + reserve cost), capital costs of conventional generating units and storages, and the gasoline cost by

Table 3.4: Peak Hour Summary and Capital Costs

Maximum Outcomes (MWh)	c1	(c2 - c1)	(c3a-c2)	(c3b-c2)	(c3c-c2)	(c3d-c2)	(c4-c2)
Conventional Generation	59,904	-4,623	-3,374	-3,445	-1,470	-2,197	-4,763
Deferrable Demand, WH	-	-	1,541	1,541	1,541	-	-
Deferrable Demand, TS	-	-	2,319	2,319	-	2,319	-
Deferrable Demand, EV	-	-	-	-	-	-	-
ESS Discharging[a]	-	-	-	-	-	-	5,667
Capital Cost ($1000)							
CG Units[b]	105,430	-8,136	-5,939	-6,064	-2,588	-3,866	-8,382
Deferrable Demand, WH[c]	-	-	397	397	397	-	-
Deferrable Demand, TS[d]	-	-	2,361	2,361	-	2,361	-
Deferrable Demand, EV[e]	-	-	5,123	-	5,123	5,123	-
ESS[e]	-	-	-	-	-	-	10,247
Total Capital Cost	105,430	-8,136	1,942	-3,306	2,932	3,619	1,864

[a] Energy Storage System (ESS)

[b] Annual capital cost for a peaker $88,000/MW/year allocated to 100 peak hours with 2 peak hours for this day

[c] Based on an installation cost of $52.8/kWh, a maintenance cost of $5/kWh-year and a 15 year life cycle

[d] Based on an installation cost of $150/kWh, a maintenance cost of $5/kWh-year and a 20 year life cycle

[e] Based on an installation cost of $900/kWh, a maintenance cost of $50/kWh-year and a 15 year life cycle

EVs. When adding wind capacity, the net savings to the total cost is approximately $20 million/day, and this value can be the reference point when making an investment decision for wind generation. However, there is still a hidden benefit from wind generation not considered here: the environment effect. One of my ongoing research studies considers the cost of fatal damage caused by emissions from conventional generating units and examines the net savings of wind generation when including the environmental cost savings.

The biggest winner among the three Case 3s and 4 is Case 3a saving approximately $6 million/day, and the large cost saving component in Case 3a is savings in the capital cost of conventional generation and gasoline cost. In fact, all Case 3s with EVs show relatively good net savings in the total system cost

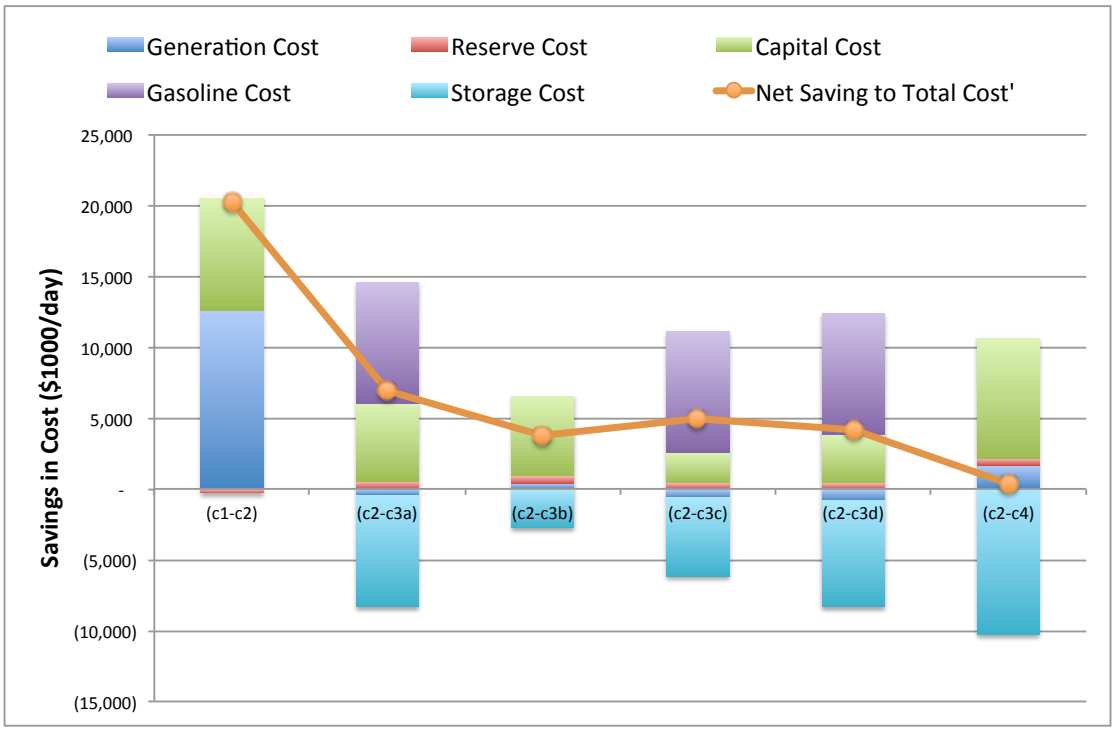

Figure 3.3: Savings in Total Cost

due to the large savings in gasoline costs even though the gasoline cost is relatively low by U.S. standards. This savings justifies the high capital cost of EV as discussed in Table 3.4. The net savings of Case 4 is the smallest among all storage cases, which is approximately $1 million/day, and it is due to the high capital cost of Lithium-Ion batteries used for ESS in this study. However, the net savings of Case 4 is still positive, and the expected storage cost reduction through technology improvement will make this net savings gradually larger in the future. Case 4 makes it clearer and more evident that there are the net positive benefits of installing ESS in the grid with a high penetration of wind generation. The cost of deferrable demand should be shared between serving its own utility and serving the grid. In this sense, the actual net savings of the total system costs for cases with deferrable demand should be higher than what

they are because the capital cost of deferrable demands for only serving the grid should be lower than what they actually are. In the current billing structure, it is difficult to realize these savings because customers who own storages do not have a billing policy that reflects this system cost. The new billing policy that reflects this system cost is introduced in the following section and analyzed for how different types of customers will be affected under this billing system.

3.4.3 Total Payments by Different Types of Customers

Based on the optimization results of Case 3a in which customers have three different types of deferrable demand, water heaters, thermal storage, and EVs, I computed the electricity bills that different types of customers need to pay under the billing policy reflecting the structure of the system costs that this study specifies. Five types of customers are defined in Case 3a. 1) Customers who do not have any deferrable demand capability, 2) Customers who own electric water heater, 3) Customers who own thermal storage for space conditioning, 4) Customers who own an EV, and 5) Customers who own all three types of deferrable demand. Customers who do not own deferrable demand capabilities are assumed to have conventional equipment to provide the same service, (e.g., customers who do not own electric water heaters with insulated tanks have just electric water heaters, and customers without thermal storage have conventional air conditioner and customers without EVs have conventional gasoline vehicles). The total number of vehicle owners in New York and New England is 15,692,624, so this number is used for the total number of customers in this region. For a better and more consistent comparison, customers are assumed to have identical hourly demand profiles for electric services: 17GWh of the to-

tal storage capacity for EVs specified in Case 3a corresponds to the aggregated storage when 10% of total customers own EVs. The same percentage of total customers own electric water heaters and thermal storage.

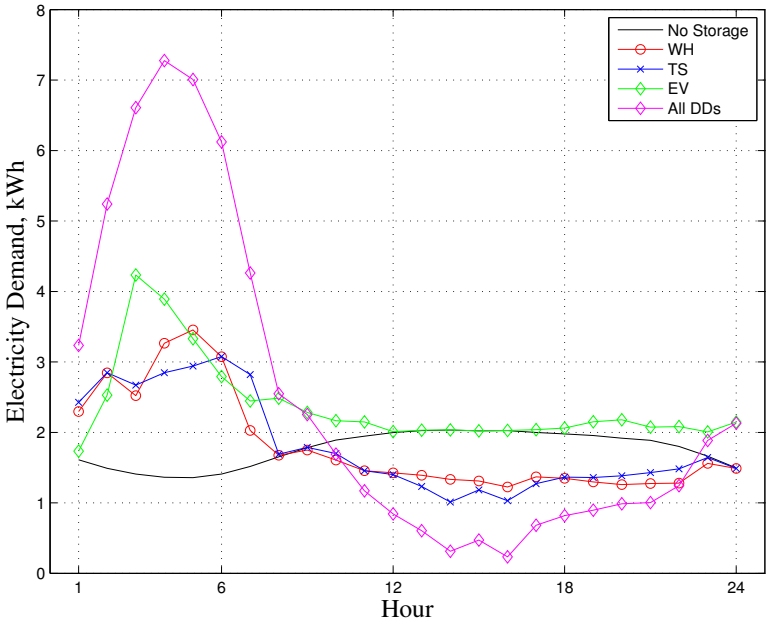

Figure 3.4: Hourly Energy Demand by Five Types of Customers

Figure 3.4 illustrates the hourly profiles of electricity purchase from the grid by five types of customers. The electricity purchase profile of customers with no storage shows the general electricity demand pattern on a hot summer day, which is low during the early morning hours and high during the hot afternoon hours. The electricity demand pattern for customers with deferrable demand capability is significantly different from the base demand profile. Customers with deferrable demand purchase significantly more electricity during the early morning hours from 1AM to 7AM when the base load is generally low and the electricity prices are at minimum levels. This additional electricity purchased is to heat up the water for the water heater, to make ice for thermal storage, and to charge up the battery for EVs. This stored energy is mainly used during

peak demand hours when electricity prices are generally high. This buy-low and sell-high mechanism allows customers with deferrable demand to make a profit, and also contributes to lowering system ramping and peak system load by flattening the daily system load throughout 24 hours.

Among the three types of deferrable demand, thermal storage contributes the most to reducing the peak demand and water heaters also show good performance in lowering the peak demand. However, EVs do not contribute to reducing the peak demand at all as V2G technology is not allowed in this study. EVs contribute to reducing the daily system ramping by filling the valley in the early morning hours. The demand profile of thermal storage is not smooth. It wiggles in the early hours and also moves up and down a little bit during the peak hours. This is because they are providing ramping services to mitigate wind variability. Customers with all three types of deferrable demand provide the biggest ramping service and contribute to reducing the peak hour demand.

To encourage customers to adopt more deferrable demand that helps reduce the overall system costs, It is important to compensate these customers with a deferrable demand with a reasonable payment scheme. The underlying rule should be that customers who contribute to reducing the system costs need to be paid for the service that they provide, and customers who incur additional costs to the system need to pay for the service that they receive. For instance, customers with deferrable demand have two kinds of electricity demand that they purchase. One is the conventional demand that they routinely purchase which is similar to the base demand profile of customers with no storage, and the other one is the deferrable demand that they purchase under the direction of the system operator under the system structure of this study. Under the rea-

sonable payment scheme, customers should pay for the ramping service that the part of conventional demand creates and get paid for providing ramping service that the part of deferrable demand contributes to. The net payment for ramping service can be positive or negative depending on how much ramping service is provided. To make this possible in reality, the smart metering needs to be implemented which records the energy purchases by conventional demand and deferrable demand separately.

Table 3.5: Composition of Payments by Five Types Of Customers

Payment($/day)	**No Storage**	**WH only**	**TS only**	**EV only**	**All DDs**
Energy Payment	3.96	3.91	3.91	5.18	5.08
Ramping Payment	0.01	-0.31	-0.37	-0.34	-1.03
Payment by CD[a]	0.01	0.05	0.04	0.05	0.13
Payment by DD[a]	-	-0.36	-0.41	-0.40	-1.17
Capacity Payment	3.58	2.35	1.78	3.58	0.55
Optimum Payment	7.55	5.94	5.32	8.42	4.59
Gasoline Payment[b]	5.44	5.44	5.44	-	-
Storage Payment[c]	-	0.25	1.50	3.26	5.02
Net Payment to Customers	12.99	11.63	12.27	11.68	9.61
Flat Payment	6.95	7.17	7.17	9.37	9.80

[a] Conventional Demand and Deferrable Demand

[b] Average daily commuting distance in urban region is 27.2 Miles and fuel efficiency is 20 Miles/Gal and gas cost considered is $4/Gal

[c] Storage Payment per cycle and per customer

Table 3.5 summarizes the composition of the optimum electricity payments for five types of customers. In addition to the base energy payment and ramping payments described above, it is assumed that customers are required to make a capacity payment which is proportional to the customer's electricity demand at a system peak load hour. For ramping payment, conventional demand (CD)

needs to pay for the ramping service that it uses, and deferrable demand (DD) gets paid for the ramping service it provides. Hence, the sum of these three components, energy payment, ramping payment, and capacity payment, is defined as an optimum payment. The energy payment of $5.18 and $5.08 for customers with EV is higher than other customers. This is because EV customers purchase more energy for commuting, but this additional energy payment is compensated by the saving in gasoline cost payment. In the ramping payment, the payment by CD is similar for all customers as they share a similar base demand profile, but the payment by DD is largely different according to each customer's deferrable demand capability. As shown in Figure 3.4, customers with all types of deferrable demand provide the most ramping service, so the payment by DD for All DDs customers is the highest negative value, $-1.17, which means that these customers get paid for the ramping service that they provide, and their net ramping payment is also negative, $-1.03. Similarly, the capacity payment of customers with all DDs is the lowest, $0.55 as they contribute the most to reducing peak demand. The customers with no storage and customers with EV show the highest capacity payment, $3.58 since EV customers do not lower the peak demand at all.

Aggregating the energy payment, ramping payment, and capacity payment, the optimum payment is the lowest for customers with all DDs and the highest for customers with EV, but considering that EV customers purchase additional energy for commuting, customers with no storage should be considered as one with the highest payments. Gasoline payment is considered for customers who do not own EVs, and the storage cost per cycle and per customer is computed to estimate the net payment of different types of customers. As illustrated in Figure 3.5, net payment to customers is computed by adding gasoline payment and

storage payment to optimum payment. The net payment is the highest for customers with no storage and lower for customers with deferrable demand, and customers with all DDs have the lowest net payment. This means that under the optimum payment scheme, customers who own many deferrable demand capabilities can save on the total net electricity payment by more than 25% compared to customers with no storage. This saving in net payment should be large enough to provide enough incentive for customers to adopt deferrable demand.

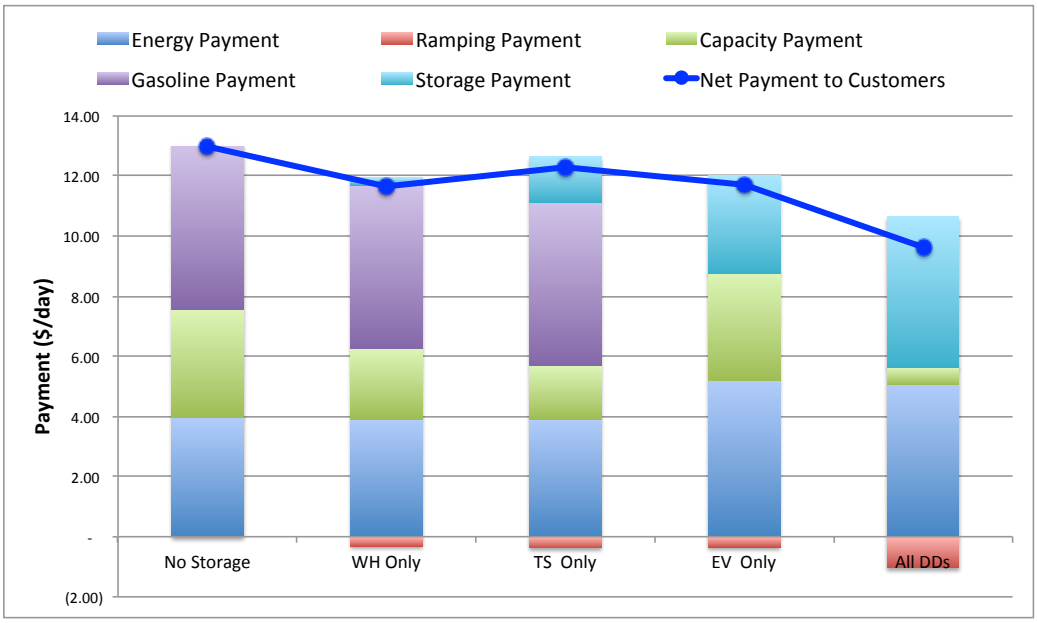

Figure 3.5: Payments by Five Types of Customers per day

Figure 3.6 illustrates the difference between optimum payment and flat payment based on the results in Table 3.5. Flat payment is the electricity payment when customers are only charged for the amount of energy purchased. This is the basic structure of the retail electricity rate that most customers in the US currently pay. The flat price applied to flat payment is determined to be 16.6 cents/kWh which is the level that makes the total revenue of the flat payment the same as the optimum payment. Under the flat payment scheme, the eco-

nomic effect of deferrable demand is perverse. Customers with deferrable demand pay more than customers with no storage, and customers with all DDs pay the most. The results of optimum payment show that the component of the largest savings in payment for customers with deferrable demand is the savings in capacity payment by getting the correct compensation for reducing peak-hour demand. The next largest saving comes from paying real-time prices for energy, and the last is getting paid for providing ramping services.

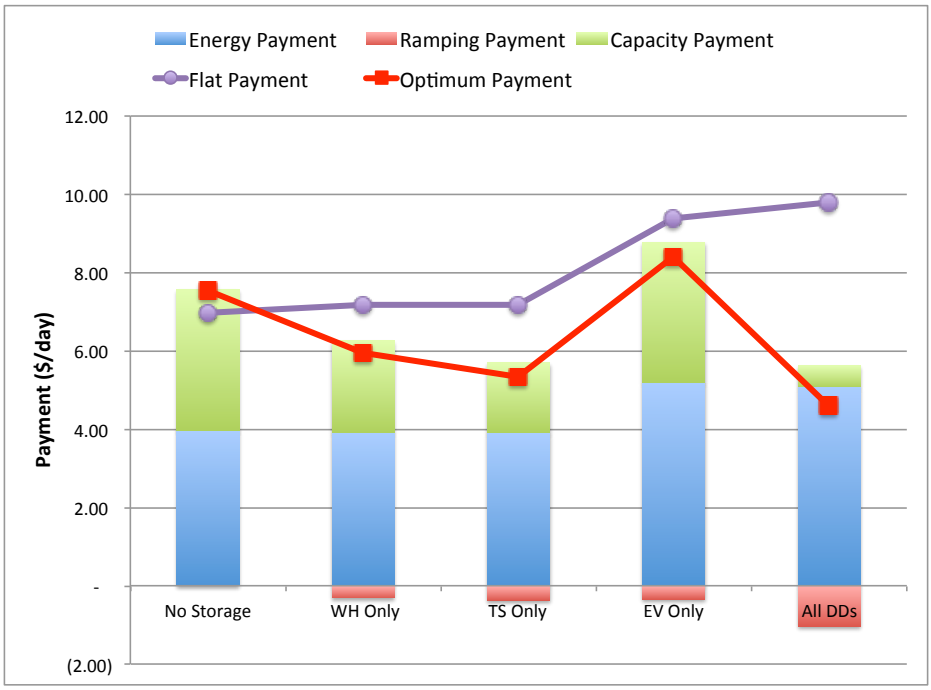

Figure 3.6: Customer's Electricity Bill Payment under Optimum Payment Scheme vs. Flat Payment Scheme

The comparison between flat payment and optimum payment highlights the problem of the current electricity rate structure. The current rate structure does not provide the appropriate economic incentives for customers to invest in the products of deferrable demand even though the benefit of deferrable demand in reducing the system costs is clear and large. In order to create more investment

in deferrable demand from customers, it is necessary to build a rate structure that makes customers pay for the service that they use and to get paid for the service that they provide.

CHAPTER 4

CONCLUSIONS AND RECOMMENDATIONS FOR REGULATORS

This study examines the effects of stochastic wind generation in the bulk power system on system costs and electricity markets, and it analyzes the true value of various types of storage from the perspectives of a system operator and of individual customers. New system cost components for ramping and storage are introduced in the model to capture the impact of highly variable wind generation, and new electricity rate structures reflecting the true system costs are introduced to determine the economically correct payments for customers who own different types of deferrable demand.

The model presented in Chapter 1 presents a simplified analysis that highlights the sensitivity of ramp-related costs associated with high wind variability, and the effect of storage in a single bus environment (i.e. with no network effects). The Chapter 2 presents the methods used to develop inputs for the model that is used for the main analysis presented in Chapter 3. This chapter describes the procedures used for modeling temperature, wind speed and electricity demand data in New York and New England, and includes the processes for selecting the sites for wind farms and demand regions, developing econometric models for forecasting hourly temperature, wind speed and the demand for electricity, illustrating the relationships among wind sites, demand regions and temperature, simulating a sample of daily realizations of wind speed and demand, transforming the forecasts of wind speed to wind power, and generating scenario profiles that represent the stochastic characteristics of wind power and electricity demand for a selected day. Chapter 2 also presents the specifications of various types of storage devices used in this study. Chapter 3 presents

an empirical analysis for a reduced model of the NPCC network representing New York State and New england, and it uses the new stochastic form of Multi-Period SuperOPF, the power system optimization platform developed at Cornell University. This empirical study is based on the information derived in Chapter 2. Chapter 3 demonstrates how a high penetration of wind generation affects the power system and the interactions between wind generation and various types of storage units. The types of storage considered include three types of deferrable demand that represent demand-side storage (electric water heaters, thermal storage for cooling, and electric vehicles (EV)), and utility-scale storage located at the wind farms. The analysis assumes that the network, including deferrable demand capacity, is managed centrally by a system operator, and it determines the optimal pattern of dispatch for generating units and storage, the impacts on the cost components of the system and on the true cost of supplying electricity to customers who own different types of deferrable demand.

Figure 4.1 illustrates the flow of information and controls between entities in the power system analyzed in Chapter 3 using the SuperOPF. The power system is centrally controlled by a system operator who manages the charging and discharging of storage and deferrable demand. Since it is unrealistic for a system operator to control the huge number of deferrable demand devices directly, it is assumed implicitly that these devices are managed by ”Passive” Aggregators using smart meters. In other words, the system operator treats each aggregator as a wholesale customer who receives instructions from the system operator about how much energy to purchase for all of their customers. The aggregator decides how to allocate this instruction among customers and their devices. The incentive for individual customers to allow aggregators access and

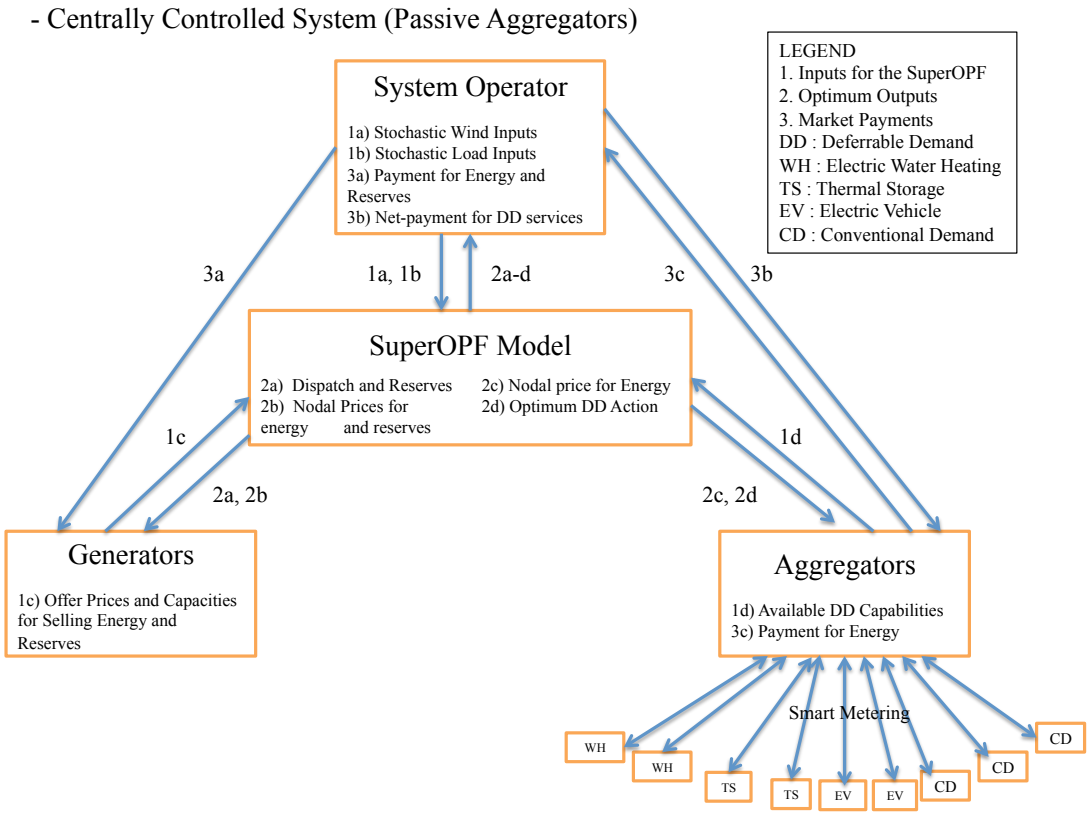

Figure 4.1: Flow Chart of Information and Controls in the Centrally Controlled Power System (Passive Aggregators)

control of their deferrable demand devices is that they will pay less but still have the same levels of energy services delivered when they want them.

The optimization process for this centrally controlled system can be categorized into three main steps. The first step is the collection of inputs for the SuperOPF from all of the entities. The system operator provides the stochastic wind and load forecasts, the generators provide their generating capacities and offer prices for energy and reserves, and the aggregators provide information regarding their aggregate demand for energy and their available deferrable de-

mand capabilities. The second step is to use the SuperOPF to determine the optimal dispatch of generating units and wind farms, and the optimal charging/discharging of storage and deferrable demand devices. Using the collected input information and other network restrictions, the SuperOPF also computes the nodal shadow prices for energy and reserves at every bus for 24 hours in all system states as well as the optimum dispatch plans. The final step is to settle the market payments for services that each entity received or provided. For generators, the system operator pays for the energy and reserves provided by them. For aggregators, the system operator receives energy payments and pays for the ramping services provided by deferrable demand.

In this passive aggregator scheme, the role of the smart meters is important. Aggregators are assumed to be connected to the individual customers by smart meters which allow them to exchange information in real time. In this centrally controlled system, the smart meters allow aggregators to access deferrable demand devices and control them following directions from the system operator. Each smart meter should be capable of metering the electricity purchased for deferrable demand devices separately from the energy used by other conventional equipment. As described in Figure 4.1, payments for energy purchased for conventional equipment are paid to the system operator separately from the net-payments for deferrable demand. In the analyses in Chapters 1 and 3, the net-payments are allocated among the customers with deferrable demand using an economically efficient billing policy that rewards, for example, the ramping services they provide and not using a traditional retail rate structure in which customers pay a flat rate for energy.

As discussed in Chapter 1 and Chapter 3, an efficient electricity rate struc-

ture should separate payments for energy, reserves and generating capacity in order to reflect the true cost of running a power system. Since the importance of a smart grid environment is growing with the increased penetration of renewable generation, the effective integration of renewable generation and the management of storage units will require the type of two-way communication system provided by smart meters. Our results show that demand-side resources provide a relatively inexpensive way to solve many of the new challenges faced by system operators compared to supply-side solutions. However, the potential benefits of demand-side solutions has not yet been widely recognized. In order to make demand-side resources, like deferrable demand, more financially attractive, I consider an efficient rate structure that charges customers for the services they use and compensates them for the services they provide is essential. Using an efficient rate structure, customers who have deferrable demand should receive substantial economic benefits by 1) purchasing more energy at less expensive off-peak prices, 2) reducing their demand during expensive peak-load periods, and 3) selling ramping services to mitigate the variability caused by renewable sources of energy.

As shown in Table 3.5, a significant portion of the savings in the net-payments made by customers with thermal storage comes from lower demand charges (by using less of the generating capacity need to meet the system peak load), and getting paid for ramping services. However, under a typical flat rate structure for energy purchases only, the positive contributions made by customers with deferrable demand to reducing system costs are not acknowledged. In fact, Figure 3.6 shows that customers with deferrable demand actually pay more than customers with no storage capabilities using a flat rate structure, and they both get the same energy services delivered. This result is

also illustrated by Figure 1.5 showing the payback periods for an initial investment in deferrable demand. Customers with thermal storage have a payback of roughly five years using an efficient rate structure but they never cover their initial investment using a flat rate structure.

However, there are still major challenges to implementing efficient rate structures in electricity markets at this time. First, it is necessary to have smart meters installed that not only share real-time information between aggregators and customers but also provide the information needed for the system operator to send instructions to aggregators for controlling deferrable demand devices optimally. For example, a demonstration project at UCLA led by Professor Rajit Gadh shows how well-designed sensors and smart meters can effectively control equipment, such as space conditioning, lights and appliances, and also incorporate the predetermined preferences of individuals and other market restrictions such as prices and power availability. Another challenge is to develop an effective method for estimating the marginal costs of energy, reserves and generating capacity for individual customers on a network with stochastic sources of renewable generation. For a system with passive aggregators, the system operator controls deferrable demand indirectly by setting an optimum dispatch plan for the total loads controlled the aggregators. It is still challenging for aggregators to determine the best way to manage the demand of individual customers and compute their net-payments in a way that is consistent with the system operator's instructions and also maintains reliability on the distribution network. Consequently, this centrally controlled system has limitations, and ideally, it would be better to develop a hierarchical system in which the system operator would provide forecasts of prices to aggregators and customers and let them decide what to do based on their own preferences, such as minimizing

the expected cost of their purchases from the grid.

One of the fundamental concepts underlying most competitive markets is that if you provide a service that increases social welfare, you should be compensated, and if you receive a service that others provide with an additional cost, you should pay for that service. This basic economic rule should apply to electricity markets. Following this rule would ensure that the markets would provide the correct economic incentives to all participants in the market. This is particularly important for encouraging the growth of deferrable demand because current retail rate structures often provde perverse economic incentives for customers to invest in deferrable demand devices. Since deferrable demand offers a relatively inexpensive way to lower system costs and deal with the variability of generation from renewable sources, the current structure of retail rates represents a major obstacle to reducing system costs. When the customers who contribute to improving the operations of a power system receive reasonable economic compensation, we will be able to build a sustainable smart grid that customers can afford.

BIBLIOGRAPHY

E. Allen, J. Lang, and M. Ilic. A combined equivalenced-electric, economic, and market representation of the northeastern power coordinating council u.s. electric power system. *Power Systems, IEEE Transactions on*, 23(3):896–907, Aug. 2008. ISSN 0885-8950. doi: 10.1109/TPWRS.2008.926715.

CAISO. Flexible resource adequacy criteria and must-oer obligation, market and infrastructure policy, fifth revised straw proposal. Technical report, California Independent System Operator (CAISO), January 2014.

H.-J. Chen, D. W. Wang, and S.-L. Chen. Optimization of an ice-storage air conditioning system using dynamic programming method. *Applied thermal engineering*, 25(2):461–472, 2005a.

J. Chen, T. D. Mount, J. S. Thorp, and R. J. Thomas. Location-based scheduling and pricing for energy and reserves: a responsive reserve market proposal. *Decis. Support Syst.*, 40(3-4):563–577, 2005b. ISSN 0167-9236. doi: http://dx.doi.org/10.1016/j.dss.2004.09.006.

S. Davis, S. Diegel, and R. Boundy. *Transportation Energy Data Book 30th Edition*. Number ORNL-5198. DOE, Oak Ridge, TN, 2011.

EAC. Bottling electricity: Storage as a strategic tool for managing variability and capacity concerns in the modern grid. Technical report, Electricity Advisory Committee, December 2008.

EIA. Household electricity reports. Technical report, U.S. Energy Information Administration (EIA), 2001.

EVAPCO. Thermal ice storage - application and design guide. Technical report, EVAPCO, Inc., 2007.

C. Gellings and W. Smith. Integrating demand-side management into utility planning. *Proceedings of the IEEE*, 77(6):908 –918, jun 1989. ISSN 0018-9219. doi: 10.1109/5.29331.

L. Goransson, S. Karlsson, and F. Johnsson. Integration of plug-in hybrid electric vehicles in a regional wind-thermal power system. *Energy Policy*, 38(10):5482–5492, Oct. 2010. ISSN 0301-4215. doi: 10.1016/j.enpol.2010.04.001.

S. Hasnain. Review on sustainable thermal energy storage technologies, part i: heat storage materials and techniques. *Energy Conversion and Management*, 39 (11):1127–1138, 1998.

B. S. Hodge, S. Huang, A. Shukla, J. F. Pekny, and G. V. Reklaitis. The effects of vehicle-to-grid systems on wind power integration in california. In S. Pierucci and G. B. Ferraris, editors, *20th European Symposium on Computer Aided Process Engineering*, volume Volume 28, pages 1039–1044. Elsevier, 2010. doi: 10.1016/S1570-7946(10)28174-9.

M. Hunt, K. Heinemeier, M. Hoeschele, and E. Weitzel. Hvac energy efficiency maintenance study. Technical report, CALMAC, 2010.

W. Jeon, J. Y. Mo, T. Mount, H. Lu, and A. J. Lamadrid. Modeling stochastic wind generation and the implications for system costs. In *The 27th Annual Western Conference, Rutgers University*, 2014.

J. Keller, D. Manz, and S. Taub. Grid scale energy storage. Technical report, General Electrics, August 2008.

A. M. Khudhair and M. M. Farid. A review on energy conservation in building applications with thermal storage by latent heat using phase change materials. *Energy conversion and management*, 45(2):263–275, 2004.

J. Kumagai. A Battery as Big as the Grid. *Spectrum*, 49(1):45–46, Jan. 2012. ISSN 0018-9235.

A. Lamadrid, S. Maneevitjit, T. Mount, C. Murillo-Sanchez, R. Thomas, and R. Zimmerman. A "superopf" framework. Technical report, CERTS, 2008.

A. J. Lamadrid, T. Mount, and W. Jeon. The effect of stochastic wind generation on ramping costs and the system benefits of storage. In *System Sciences (HICSS), 2013 46th Hawaii International Conference on*, pages 2271–2281, 2013. doi: 10.1109/HICSS.2013.631.

A. J. Lamadrid, T. D. Mount, W. Jeon, and H. Lu. Is deferrable demand an effective alternative to upgrading transmission capacity? *Journal of Energy Engineering*, 2014.

W.-S. Lee, Y.-T. Chen, and T.-H. Wu. Optimization for ice-storage air-conditioning system using particle swarm algorithm. *Applied Energy*, 86(9): 1589–1595, 2009.

S. A. Lefton, P. M. Besuner, and D. D. Agan. The real cost of on/off cycling. *Modern power systems*, 26(10):11 @ 0260–7840, 2006.

M. MacCracken. Energy storage providing for a low-carbon future. *ASHRAE Journal*, 52(9), 2010.

MassDiv. Installation guide for electric vehicle charging equipment. Technical report, The Massachusetts Division of Energy Resources, 2000.

J. Y. Mo. *Economic Analyses of Plug-in Hybrid Electric Vehicles, Carbon Markets, and Temperature-Sensitive Loads*. PhD thesis, Cornell University, 2012.

P. Norgaard and H. Hottlinen. A multi-turbine power curve approach. In *Nordic Wind Power Conference*, pages 1–5, 2004.

B. Q. Parsons and Douglas. Regional travel - household interview survey. Technical report, The New York Metropolitan Transportation Council, the North Jersey Transportation Planning Authority, 2000.

K. Pennock. Updated eastern interconnect wind power output and forecasts for ergis. Technical report, NREL, October 2012.

F. Schweppe, B. Daryanian, and R. Tabors. Algorithms for a spot price responding residential load controller. *Power Systems, IEEE Transactions on*, 4(2):507 –516, may 1989. ISSN 0885-8950. doi: 10.1109/59.193823.

A. Sharma, V. V. Tyagi, C. R. Chen, and D. Buddhi. Review on thermal energy storage with phase change materials and applications. *Renewable and Sustainable Energy Reviews*, 13(2):318–345, 2 2009. doi: http://dx.doi.org/10.1016/j.rser.2007.10.005.

W. Short and P. Denholm. *Preliminary Assessment of Plug-in Hybrid Electric Vehicles on Wind Energy Markets*. National Renewable Energy Laboratory, 2006.

R. Sioshansi and P. Denholm. The value of plug-in hybrid electric vehicles as grid resources. *The Energy Journal*, 31:1–22, 2010.

R. Thomas, C. Murillo-Sanchez, and R. Zimmerman. An advanced security constrained opf that produces correct market-based pricing. In *Power and Energy Society General Meeting - Conversion and Delivery of Electrical Energy in the 21st Century, 2008 IEEE*, pages 1–6, July 2008. doi: 10.1109/PES.2008.4596331.

N. Troy. *Generator cycling due to high penetrations of wind power*. University College Dublin, Ireland, 2011.

A. Tuohy and M. O'Malley. Pumped storage in systems with very high wind penetration. *Energy Policy*, 39(4):1965–1974, Apr. 2011. ISSN 0301-4215. doi: 10.1016/j.enpol.2011.01.026.

K. Valentine, W. G. Temple, and K. M. Zhang. Intelligent electric vehicle charging: Rethinking the valley-fill. *Journal of Power Sources*, 196(24):10717–10726, Dec. 2011. ISSN 0378-7753. doi: 10.1016/j.jpowsour.2011.08.076.

J. Wang, D. Ryan, and E. J. Anthony. Reducing the greenhouse gas footprint of shale gas. *Energy Policy*, 39(12):8196 – 8199, 2011. ISSN 0301-4215. doi: 10.1016/j.enpol.2011.10.013. Clean Cooking Fuels and Technologies in Developing Economies.

R. D. Zimmerman, C. E. Murillo-Sanchez, and R. J. Thomas. Matpower: Steady-state operations, planning, and analysis tools for power systems research and education. *Power Systems, IEEE Transactions on*, 26(1):12 –19, 2011. ISSN 0885-8950. doi: 10.1109/TPWRS.2010.2051168.